

VARIATIONS

Spring 2016 • Vol. 14, No. 2

A Tale of Two Blobs

Editors:

Kristan Uhlenbrock &
Mike Patterson

From 2013 to 2015, the scientific community and the media were enthralled with two anomalous sea surface temperature events, both getting the moniker the “Blob,” although one was warm and one was cold. These events occurred during a period of record-setting global mean surface temperatures. This edition focuses on the timing and extent, possible mechanisms, and impacts of these unusual ocean heat anomalies, and what we might expect in the future as climate changes.

The “Warm Blob” feature appeared in the North Pacific during winter 2013 and was first identified by Nick Bond, University of Washington. This record-breaking event remained through 2015, morphing in shape and causing widespread impacts on the marine ecosystem. Scientists are still answering questions such as whether the warm blob could have played a role in the strong 2015-16 El Niño event and whether these multi-year climate extremes (e.g., marine heatwaves) will become more frequent in a warming climate.

The North Atlantic experienced a record-breaking cold ocean

The evolution and known atmospheric forcing mechanisms behind the 2013-2015 North Pacific warm anomalies

Dillon J. Amaya¹ Nicholas E. Bond²,
Arthur J. Miller¹, and Michael J. DeFlorio³

¹Scripps Institution of Oceanography

²University of Washington

³Jet Propulsion Laboratory, California Institute of Technology

Year-to-year variations in the El Niño Southern Oscillation (ENSO) indices generate significant interest throughout the general public and the scientific community due to the sometimes destructive nature of this climate mode. For example, so-called “Godzilla” ENSOs can generate billions of dollars in damages from the US agricultural industry alone due to unanticipated flooding or drought (Adams et al. 1999). However, in the winter of 2013/2014, North Pacific sea surface temperature (SST) anomalies exceeded three standard deviations above the mean over a large region, shifting focus away from the tropics and onto the extratropics as the associated atmospheric circulation patterns helped exacerbate the most significant California drought in the instrumental record (Swain et al. 2014; Griffin and Anchukaitis 2014). This extratropical warming has since become known in the media and the literature simply as “the Blob” or “the Warm Blob” and represents a climate state unlike anything seen in the last 30 years (Figure 1; Bond et al. 2015).

IN THIS ISSUE

The evolution & known atmospheric forcing mechanisms behind the 2013-15 North Pacific warm anomalies	1
Impact of the Blob on the Northeast Pacific Ocean biogeochemistry & ecosystems	7
Climate interpretation of the North Pacific marine heatwave of 2013-15	13
The tale of a surprisingly cold blob in the North Atlantic	19
What caused the Atlantic cold blob of 2015	24
Greenland Ice Sheet melting influence on the North Atlantic	32

surface temperature, dubbed the “Cold Blob,” during 2015 in a region southeast of Greenland. This surface layer cooling has been mostly attributed to air-sea heat loss and ocean heat content anomalies. However, how it formed and if it will stay is still up for debate. The Atlantic Meridional Overturning Circulation may play a role, as well as the decadal variability of the North Atlantic Oscillation. Scientists are also looking into whether meltwater from the Greenland ice sheet could influence and cold blob, with modeling results presented herein suggesting that it doesn’t.

The series of articles in this edition highlight research of the North Pacific warm blob—featuring contributions by Amaya et al., Siedlecki et al., and Di Lorenzo et al.—and the North Atlantic cold blob—featuring contributions by Duchez et al., Yeager et al., and Schmittner et al. This collection aims to highlight recent work, theories, and advancements in understanding these phenomena with an aim to stimulate discussion within the community. To facilitate this, a series of webinars will be hosted with the authors in June, with more information found on [page 38](#).

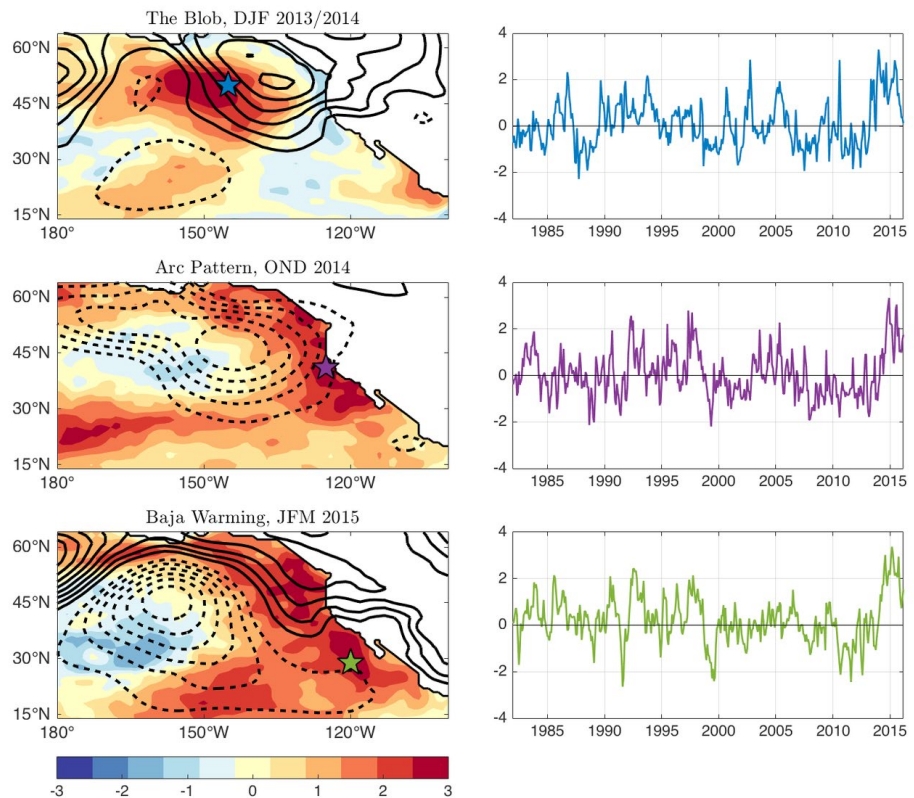


Figure 1. Normalized SST anomalies (shading) and SLP anomalies in millibars (contours) averaged over December–February (DJF) 2013/2014 (top row), October–December (OND) 2014, and January–March (JFM) 2015. Positive SLP values are solid contours, negative values are dashed, and the contour interval is 1 mb. Colored stars indicate the point location for the respective SST anomaly time series found to the right of each map. SST data for this figure are from NOAA Optimally Interpolated Sea Surface Temperature Version 2 (OISSTv2), and SLP data are from NCEP/NCAR Reanalysis.

The Warm Blob is both unprecedented in magnitude and remarkably persistent as it has hung around in various shapes and sizes since that first winter of 2013/2014 to the present. Godzilla El Niño will at least decay within a year, but the Warm Blob’s lingering effects have raised concerns for our understanding of the region, our ability to predict future such events, and the role of anthropogenic climate change in maintaining North Pacific warming. Here, we present a synthesis of what is currently known about the Warm Blob with respect to its historical magnitude and persistence.

“Doctor, nothing will stop it!”-The Blob (1958)

The conundrum that the Warm Blob presents is due, in part, to the fact that the center of action during the winter of 2013/2014 is only one part of a larger story. In reality, the North Pacific Blob has evolved in space over the course of the last three years, growing and decaying between three different centers of action each with three distinct forcing mechanisms. Normalized SST anomalies in the North Pacific for select seasons from 2013–2015 are shown in Figure 1. The canonical Blob first

US CLIVAR VARIATIONS

Editors: Mike Patterson and Kristan Uhlenbrock
US CLIVAR Project Office
1201 New York Ave NW, Suite 400
Washington, DC 20005
202-787-1682 | www.usclivar.org
© 2016 US CLIVAR

described by Bond et al. (2015) can be seen in the first row. The blue star marks the location of the Warm Blob time series on the right. Based on this curve and the work of several studies (e.g., Bond et al. 2015; Di Lorenzo and Mantua 2016) the Warm Blob is the largest Northeast Pacific SST anomaly seen in at least the last 30 years.

Sea level pressure (SLP) anomalies (black contours) outline a ridge of high-pressure on the eastern flank of the Warm Blob that exhibited strong persistence throughout much of 2013 and 2014, earning it the moniker, "Ridiculously Resilient Ridge" (hereafter called the Ridge). This Ridge caused persistent deflections of wintertime storms north of California, enhancing and sustaining drought conditions in the region (e.g., Swain et al. 2014). Additionally, downstream perturbations to the jet stream associated with the persistence of the Ridge helped generate the historically cold winter season across North America in 2013/2014 (Hartmann 2015). Various hypothesis have been proposed to explain the Ridge's resiliency,

including remote teleconnections driven by warmer than normal conditions in the western tropical Pacific, which may have led to significant extratropical ocean-atmosphere feedbacks (Wang et al. 2014; Hartmann 2015; Lee et al. 2015; Seager et al. 2015). Another possibility is the influence of Arctic sea ice loss on North Pacific geopotential height fields through various thermal effects (Lee et al. 2015; Sewall and Sloan 2005; Kug et al. 2015). Atmospheric internal variability could have also played a role (Seager et al. 2015).

Regardless of the specific factors determining its genesis, the Ridge is the driving force behind our first center of action—the Blob (Figure 1, top row). The results of a mixed layer heat budget conducted by Bond et al. (2015) over the Warm Blob region are depicted in Figure 2. They show that the anticyclonic flow around the Ridge significantly reduced the strength of the background westerlies, which limited the amount of energy imparted by the atmosphere into the ocean for mixing processes. As a result, Bond et al. (2015) observed enhanced mixed layer stratification, decreased advection of cold water from the Bering Sea, reduced vertical entrainment of cold waters from below, and limited seasonal cooling of the upper ocean (Figure 2). These results highlight the fact that the Warm Blob owes its existence not to processes that actively warmed the mixed layer, but simply due to a lack of wintertime cooling in 2013/2014.

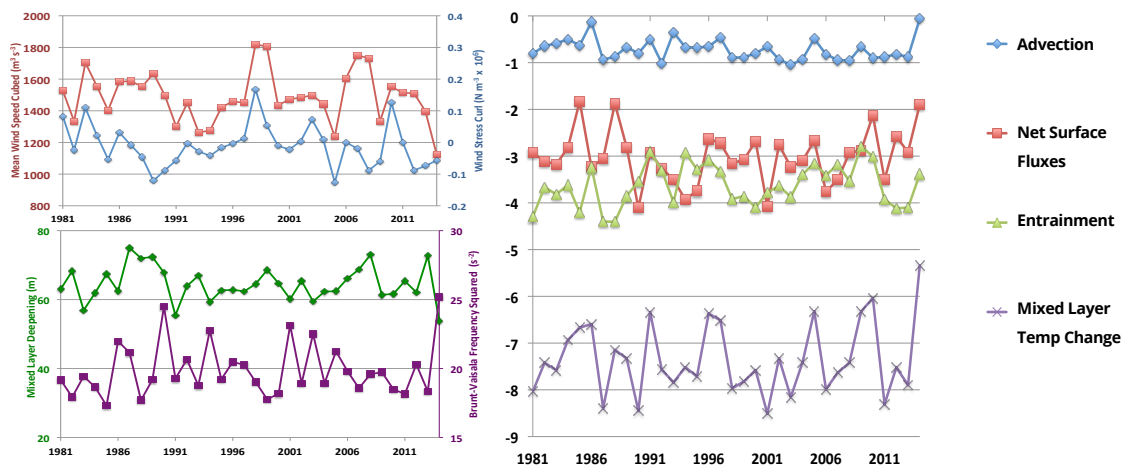


Figure 2. (top, left) Time series of seasonal mean (October–January) wind speed cubed (red) and wind stress curl (blue) for the area of 50–40°N, 150–135°W. (bottom, left) Time series of mean seasonal mixed layer deepening (September–February; green) and stratification at the base of the mixed layer (February; purple) for the area of 50–40°N, 150–135°W. The years refer to averaged January–February values. (right) Seasonal values of the mixed layer temperature change from September to February for the area of 50–40°N, 150–135°W (purple) and budget terms contributing to this temperature change. Budget terms include horizontal advection (blue), net surface heat fluxes (red), and entrainment (light green). Values represent temperature change (°C) associated with the individual terms. Adapted from Bond et al. (2015).

A shift in forcing mechanisms

In early 2014 nearly every forecasting model predicted the arrival of a significant El Niño in the following winter. However, by the fall it became evident that the weak warming along the equatorial strip was not going to amplify into a major warm event. Even though the 2014/2015 El Niño fizzled out early, a recent study by Di Lorenzo and Mantua (2016) indicates that this equatorial warming may have been enough to produce a positive state of the Pacific North American (PNA) pattern, and in particular a relatively deep and southeast displaced Aleutian Low (Figure 1, second row). By breaking down the Ridge, the “El Niño that wasn’t” altered the atmospheric forcing driving North Pacific warming the previous winter, and allowed the Warm Blob to evolve into something else entirely—the Arc Pattern.

In contrast to the more offshore Blob, the Arc Pattern is characterized by broad coastal warming, reminiscent of a Pacific Decadal Oscillation (PDO)-like structure (Figure 1, second row). The “arrival” of the Warm Blob onshore had substantial consequences for regional ecosystems in Gulf of Alaska all the way to the Baja California Peninsula ([see Siedlecki et al., this issue](#)) and also represented a 30-year record warming along the coast (Figure 1, second row). However, the preliminary research outlined above indicates that the Arc Pattern is not the result of the Warm Blob “moving” or advecting onshore, but rather a consequence of an entirely different forcing mechanism. Di Lorenzo and Mantua (2016) advance this theory by showing that a simple one-dimensional auto-regressive model based on a short-term memory of the SST and the altered SLP anomaly pattern in fall 2014 (deepened Aleutian low) can accurately reproduce the Arc Pattern warming.

In addition, Zaba and Rudnick (2016) used underwater glider data to suggest that the anomalous cyclonic circulation during this time period weakened the climatological upwelling favorable winds along the California coastline, which then suppressed upper ocean mixing and seasonal upwelling. Their observations indicated that once positive SST anomalies were

established, a reduction in low-level cloud cover may have enhanced downward shortwave radiation at the surface, resulting in more SST warming and a positive feedback (Zaba and Rudnick 2016; Schwartz et al. 2014). While these results are primarily associated with the Southern California Current System, they illustrate the importance of different atmospheric forcing mechanisms in facilitating the transition from the Warm Blob to the Arc Pattern.

Baja warming and Godzilla El Niño

With 2014 drawing to a close, all signs once again pointed to the possibility of a strong El Niño in the following winter. The Aleutian Low maintained negative anomalies into early 2015, possibly as a result of these continued El Niño-like conditions. However, during the first few months of 2015, anomalously low pressures dipped further south and east into the tropics. This would tend to produce surface wind anomalies that opposed the climatological trade winds below 30°N. Consequently, reduced evaporative cooling at the surface would drive a heat flux into the ocean and shift the center of action for North Pacific warming southward, off the coast of the Baja California Peninsula (Figure 1, last row). The transition to the Baja Warming Pattern is further highlighted by the three time series depicted in Figure 1. When the Baja Warming time series reaches a 30-year peak in January–March (JFM) 2015, the Arc Pattern time series sharply decreases to less positive values. To date, there is little published research on the transition from the Arc Pattern to Baja warming. Therefore, the mechanisms outlined above and to follow are merely the conjectures of the authors, and we encourage future study on the topic.

The Baja Warming Pattern has similar spatial characteristics to the Pacific Meridional Mode (Chiang and Vimont 2004). Thus, it is likely that air-sea interactions like the wind-evaporation-SST feedback and/or the low-level cloud/SST feedback play significant roles in maintaining the broad nature of the Baja Warming Pattern (e.g., Chiang and Vimont 2004; Di Lorenzo and Mantua 2016). Similarly, there are indications from preliminary results presented at the [Pacific Anomalies Workshop II](#), held this

January at the University of Washington, that coastally trapped Kelvin waves generated during the formation of the 2015/2016 El Niño may have contributed to the warming along the coastline of Mexico by suppressing upwelling. This signal could then propagate westward as Rossby waves and potentially enhance the broader-scale warming seen in Figure 1.

A final separate but related question would be, what was the role of the Baja Warming in generating the Godzilla El Niño of 2015/2016 in the first place? Feng et al. (2014) and others argue that SST anomalies off the coast of Baja California can act as a possible precursor of ENSO through the dynamics associated with the Pacific Meridional Mode. It is therefore possible that the Baja Warming Pattern, which had its origins in the Arc Pattern, helped drive the formation of a significant El Niño in 2015 that then could have potentially reinforced the Baja Warming further via the coastally trapped Kelvin waves.

The end of the Blob?

As predicted by nearly every model, the late 2015-early 2016 El Niño was one of the strongest tropical Pacific SST warming events ever captured by the instrumental record. This increased warming and associated strengthening in deep convection teleconnected to the North Pacific and helped deepen the Aleutian Low and drive the steady decline of the North Pacific warming features described previously. The JFM 2016 average SST and SLP anomalies in the North Pacific are shown in Figure 3. Here, we see the anomalous low-pressure center driving a PDO-like pattern of SST anomalies, with cold anomalies in the central North Pacific and warming along the southern, eastern, and northern edges of the Aleutian Low. These anomalies are most likely due to anomalous wind driven heat fluxes

at each of these locations (e.g., Alexander and Scott 1997). As a result of this forcing, the Gulf of Alaska warming associated with the Blob has decayed to neutral values while the Arc Pattern and Baja Warming have weakened substantially (Figure 1, timeseries).

Is the Warm Blob gone for good? Based on current observations, this seems to be the case, at least for now. The anomalous warming in the Gulf of Alaska has weakened and then experienced a significant resurgence once before, from late 2014 to early 2015 (Figure 1), so it is difficult to make a prediction with high certainty. In particular, anomalously warm water below the mixed layer, as indicated by ARGO (not shown) suggests that the thermal “inertia” of this region may be especially high. Additionally, mid-April model projections suggest there is a 60% chance of La Niña conditions in the equatorial Pacific by the winter of 2016/2017 ([CPC/IRI Probabilistic ENSO Forecast](#)). La Niña tends to produce opposite signed anomalies in the Aleutian Low, and if the Ridge was the driving force of the Warm Blob in 2013/2014, then it is possible a La Niña-driven high-pressure anomaly over the Gulf of Alaska may give the Blob new life.

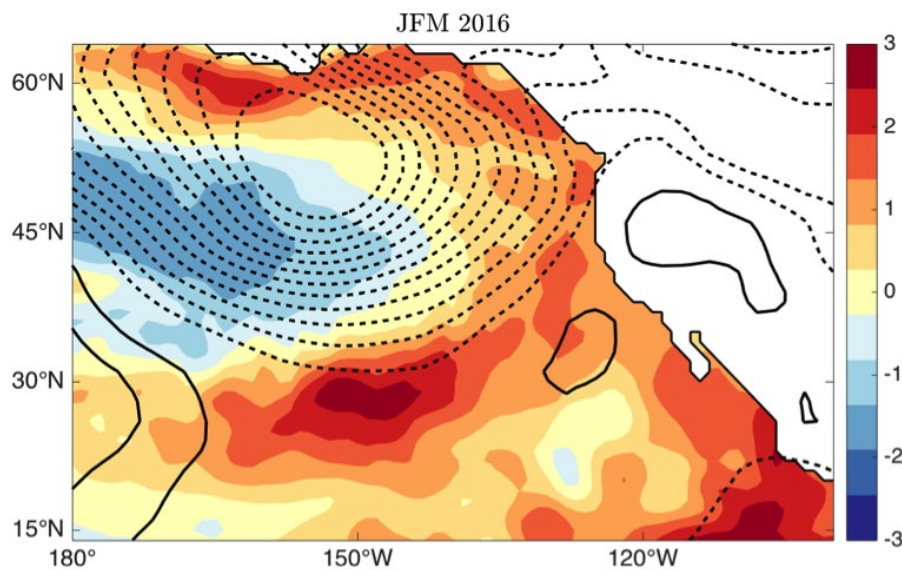


Figure 3: As in Figure 1, but SST and SLP anomalies are averaged from January-March (JFM) 2016. Data sources same as in Figure 1.

The warm anomalies throughout the Pacific from 2013 to present have been truly historic and have provided us with a significant opportunity to explore extratropical oceanic heat waves like never before due to the high spatiotemporal density of modern-day observational networks. We encourage future investigation into each of the centers of action described in this article, as well as a stronger focus on the role of the ocean-atmosphere

interactions that may have led to transitions between them. As discussed in a later article these types of events may become more frequent in a changing climate. Therefore, it is of high socioeconomic concern to understand these phenomena moving forward.

References

- Adams, R. M., C. C. Chen, B. McCarl, and R. Weiher, 1999: The economic consequences of El Niño and La Niña events for agriculture. *Improving El Niño Forecasting: The Potential Economic Benefit*. R. Weiher, Ed., 15-20.
- Alexander, M. A., and J. D. Scott, 1997: Surface flux variability over the North Pacific and North Atlantic Oceans. *J. Climate*, **10**, 2963–2978, doi:[10.1175/1520-0442\(1997\)010<2963:SFVOTN>2.0.CO;2](https://doi.org/10.1175/1520-0442(1997)010<2963:SFVOTN>2.0.CO;2).
- Bond, N. E., M. F. Cronin, H. Freeland, and N. Mantua, 2015: Causes and impacts of the 2014 warm anomaly in the NE Pacific. *Geophys. Res. Lett.*, **42**, 3414–3420, doi:[10.1002/2015GL063306](https://doi.org/10.1002/2015GL063306).
- Chiang, J. C., and D. J. Vimont, 2004: Analogous Pacific and Atlantic meridional modes of tropical atmosphere-ocean variability. *J. Climate*, **17**, 4143–4158, doi: [10.1175/JCLI4953.1](https://doi.org/10.1175/JCLI4953.1).
- Di Lorenzo, E., and N. J. Mantua, 2016: Multi-year persistence of the 2014/15 North Pacific marine heatwave. *Nat. Climate Change*, accepted.
- Feng, J., Z. Wu, and X. Zou, 2014: Sea surface temperature anomalies off Baja California: A possible precursor of ENSO. *J. Climate*, **71**, 1529–1537, doi: [10.1175/JAS-D-13-0397.1](https://doi.org/10.1175/JAS-D-13-0397.1).
- Griffin, D., and K. J. Anchukaitis, 2014: How unusual is the 2012–2014 California drought? *Geophys. Res. Lett.*, **41**, 9017–9023, doi:[10.1002/2014GL062433](https://doi.org/10.1002/2014GL062433).
- Hartmann, D. L., 2015: Pacific sea surface temperature and the winter of 2014. *Geophys. Res. Lett.*, **42**, 1894–1902, doi:[10.1002/2015GL063083](https://doi.org/10.1002/2015GL063083).
- Kug, J.-S., J.-H. Jeong, Y.-S. Jang, B.-M. Kim, C. K. Folland, S.-K. Min, and S.-W. Son, 2015: Two distinct influences of Arctic warming on cold winters over North America and East Asia. *Nat. Geosci.*, **8**, 759–762, doi:[10.1038/ngeo2517](https://doi.org/10.1038/ngeo2517).
- Lee, M.-Y., C.-C. Hong, and H.-H. Hsu, 2015: Compounding effects of warm sea surface temperature and reduced sea ice on the extreme circulation over the extratropical North Pacific and North America during the 2013–2014 boreal winter. *Geophys. Res. Lett.*, **42**, 1612–1618, doi:[10.1002/2014GL062956](https://doi.org/10.1002/2014GL062956).
- Schwartz, R. E., A. Gershunov, S. F. Iacobellis, and D. R. Cayan, 2014: North American west coast summer low cloudiness: Broadscale variability associated with sea surface temperature. *Geophys. Res. Lett.*, **41**, 3307–3314, doi: [10.1002/2014GL059825](https://doi.org/10.1002/2014GL059825).
- Seager, R., M. Hoerling, S. Schubert, H. Wang, B. Lyon, A. Kumar, J. Nakamura, and N. Henderson, 2015: Causes of the 2011–14 California Drought. *J. Climate*, **28**, 6997–7024, doi:[10.1175/JCLI-D-14-00860.1](https://doi.org/10.1175/JCLI-D-14-00860.1).
- Sewall, J. O., and L. C. Sloan, 2005: Disappearing Arctic sea ice reduces available water in the American west. *Geophys. Res. Lett.*, **31**, L06209, doi:[10.1029/2003GL01913](https://doi.org/10.1029/2003GL01913).
- Swain, D. L., M. Tsiang, M. Haugen, D. Singh, A. Charland, B. Rajaratnam, and N. S. Diffenbaugh, 2014: *The extraordinary California drought of 2013/2014: Character, context, and the role of climate change*. [in "Explaining Extremes of 2013 from a Climate Perspective]. *Bull. Am. Meteorol. Soc.*, **95**, S3–S7.
- Wang, S.-Y., L. Hipps, R. R. Gillies, J.-H. Yoon, 2014: Probable causes of the abnormal ridge accompanying the 2013–2014 California drought: ENSO precursor and anthropogenic warming footprint. *Geophys. Res. Lett.*, **41**, 3220–3226, doi: [10.1002/2014GL059748](https://doi.org/10.1002/2014GL059748).
- Zaba, K. D., and D. L. Rudnick, 2016: The 2014–2105 warming anomaly in the Southern California Current System observed by underwater gliders. *Geophys. Res. Lett.*, **43**, 1241–1248, doi:[10.1002/2015GL067550](https://doi.org/10.1002/2015GL067550).

Impact of the Blob on the Northeast Pacific Ocean biogeochemistry and ecosystems

Samantha Siedlecki¹, Eric Bjorkstedt^{2,3}, Richard Feely⁴, Adrienne Sutton^{1,4}, Jessica Cross⁴, and Jan Newton¹

¹University of Washington

²National Marine Fisheries Service, NOAA

³Humboldt State University

⁴Pacific Marine Environmental Laboratory, NOAA

During winter 2013-14, a region of unusually warm water now commonly referred to as the Blob (Bond et al. 2015) emerged in the North Pacific, due to a persistent high-pressure ridge that inhibited winter mixing, thus preventing typical cooling of surface waters. This physical disturbance persisted for more than a year and was associated with the strongest North Pacific Ocean warming of a non-El Niño pattern. The Blob was first apparent in the Gulf of Alaska (GOA), and then was evident off the US West Coast, where it intersected with the coastal California Current System (CCS).

While the physical disturbance into 2016 was compounded by another anomalously warm set of conditions driven by El Niño, the biogeochemical and ecosystem ramifications are still being sorted out and will likely remain impacted for years to come. This is a result of the important role temperature plays in biogeochemical cycles and ecosystem dynamics.

Temperature largely determines what biogeochemists call the solubility pump for carbon in the ocean. The solubility pump transports carbon from the ocean's surface to the deep interior as dissolved inorganic carbon. The same solubility pump affects all gases in the ocean

to various degrees. For oxygen and carbon, the solubility is a strong inverse function of temperature, such that cold water has the greater capacity to hold more gas. This mostly impacts the gas concentrations and fluxes at the surface, but the signal is propagated through mixing downwards throughout the water column. Oxygen equilibrates quickly with the atmosphere, but carbon takes longer (~1 year). All of these processes combined result in outgassing for carbon and oxygen from the warming.

NOAA's Pacific Marine Environmental Laboratory (PMEL) has been monitoring sea surface CO₂ concentrations in the Pacific since 1982, including underway pCO₂ systems on six different container ships, which document changes in surface pCO₂ across the Pacific basin. One transect line traveled through the Blob region (15°N to 35°N). In that region, the decadal increase in pCO₂ values reached up to 49 μatm, which constitutes a 47% enrichment in pCO₂ due to the anomalously warm waters relative to the decadal change. This enhanced carbon source may have strong implications for the oceanic carbon budget during the Blob's existence, and has the potential to transition this region of the Northeast Pacific from a CO₂ sink to a CO₂ source (Cosca et al. 2016). Because CO₂ has a long

equilibration time with the atmosphere, the impact from the Blob's anomalous temperatures on carbon will persist beyond the temperature anomaly for several months.

Temperature changes also alter the stratification of the water column, which alters the vertical exchange of nutrients, oxygen, and carbon throughout. In the case of the Blob, the temperature anomaly was seen up to 50 meters below the surface, so it follows that the biogeochemical properties were altered below the surface as well. The nutrient-rich, carbon-rich, oxygen-depleted waters were most likely suppressed deeper in the Blob region. As a result of more intense stratification and altered isopleths, upwelling—while evident during both 2014 and 2015—yielded different surface conditions along the CCS and within coastal regions like the GOA during the presence of the Blob. While upwelling along the CCS kept the Blob conditions offshore during summer 2014, in 2015 this was not the case. From remote sensing and buoy observations, we see that late summer (July, August) upwelling was associated with warmer than normal surface temperatures and presumably more Blob-affected water chemistry.

The CCS is a highly productive upwelling regime susceptible to ocean acidification and hypoxia. Additionally, temperature can impact ecosystems in several important ways including defining habitats, cuing reproduction, and influencing metabolism, life cycles, and behavior. The Blob's temperature anomaly, thus, has strong potential to have affected ecosystems, including fisheries and zooplankton species that are important for fish. Both the GOA and CCS support economically important fisheries, together grossing more than a billion dollars a year (NMFS 2014). The impacts of the Blob on fisheries are still being quantified, as some remain closed.

The biogeochemistry of the Blob on the coastal ocean

CO₂ in the Gulf of Alaska and California Current System

In contrast to the open ocean Blob, observations in coastal regions show a different trend. In the GOA, along the Seward Line, pCO₂ concentrations near the surface were lower than the prior six years. In the GOA, a known sink for atmospheric CO₂, the strength of the sink to the atmosphere may have increased during this interval. Further south, in the CCS (Figure 1), the surface pCO₂ values were reduced as well, but not as dramatically as in the GOA. The pCO₂ near the surface at Cape Elizabeth in Washington was much lower in the fall of 2014 when the Blob arrived on the coast than the prior years of observation. The following spring continued to be low, but by mid-summer, the pCO₂ near the surface values returned to mid-range. The observations in the Southern California region indicate different pCO₂ trends in 2014–2015 than the observations off the Washington coast, indicating that some regional processes are generating

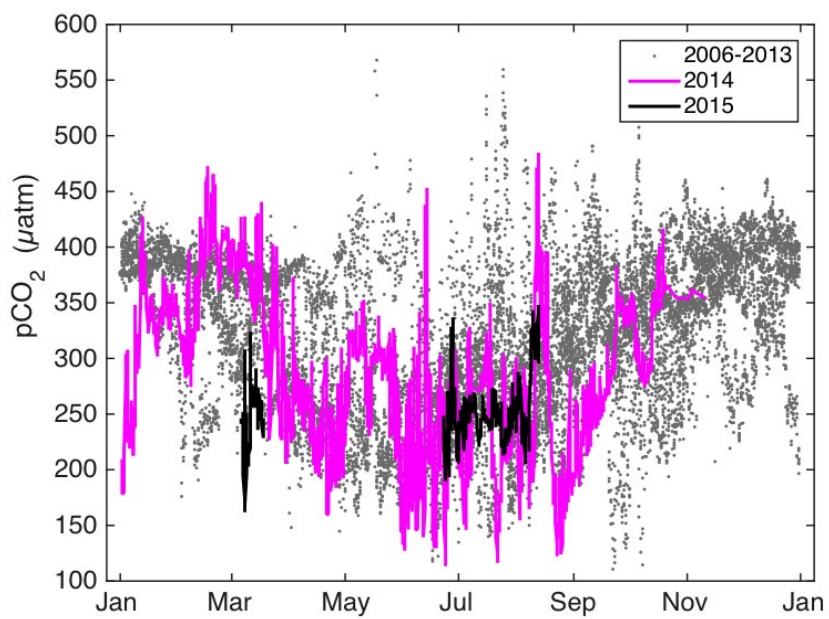


Figure 1: Surface pCO₂ concentrations in μatm from a mooring in Washington (Cape Elizabeth, 42 m depth, 2006–2015). Grey dots represent all data taken from 2006–2013; pink line shows data from 2014; black line shows data from 2015. Finalized data are available on the [CDIAC website](#).

spatial variability of the magnitude of the signal along the CCS. Possible mechanisms include capped upwelling of pCO₂ rich deep waters, anomalously high primary production (as was the case in 2015), or some combination of the two resulting in lower surface pCO₂ concentrations.

Ocean Acidification in the coastal regions

In the GOA, the Seward Line carbon chemistry observations have been made since 2008. Aragonite saturation state (Ω ; $\Omega_a < 1$ indicates undersaturation) measures the state of conditions for precipitation of aragonite (a more soluble form of CaCO₃) in seawater. Certain marine organisms, including oysters, precipitate shells made out of CaCO₃. Values below one indicate undersaturation, and dissolution is favored. For some organisms, like juvenile oysters, sensitivity and even decreased survival has been exhibited in lab experiments for values above the physical chemistry threshold of one (Waldbusser et al. 2015). In 2014 and 2015, the unusually warm and persistently fresh conditions produced low dissolved inorganic carbon/total alkalinity (DIC/TA) ratios. As a result, unusually high aragonite saturation states ($\Omega_a \approx 3$) developed at the surface and extended down nearly 200 meters (Figure 2).

In the CCS, the pH trends were similar to the pCO₂ trends described above: The pH increases slightly in 2015 relative to 2014. These conditions provide a reprieve for calcifying organisms from the undersaturated and corrosive conditions common in the CCS in recent years (Feely et al. 2008).

Oxygen on the shelf in the CCS

During the fall of 2014 when the Blob came onshore in Washington, near bottom oxygen values were higher than observed oxygen levels since 2006 (Figure 3a). In 2015, the bottom oxygen levels were higher than the previous

years in June, became lower in July, and finished the season with higher bottom oxygen than prior years. Further south, near bottom oxygen at the Trinidad Head Line (station TH02; 41°03.5'N, 124°16'W; 75 m depth) was higher than average for both years over much of the upwelling season, consistent with regions further north (Leising et al. 2015; Figure 3b). In the CalCOFI region (the coastal region located off of southern California), along the density surface 26.5 kg m⁻³, oxygen concentrations were closer to the average value for the area for both years (Leising et al. 2015; Figure 3c,d).

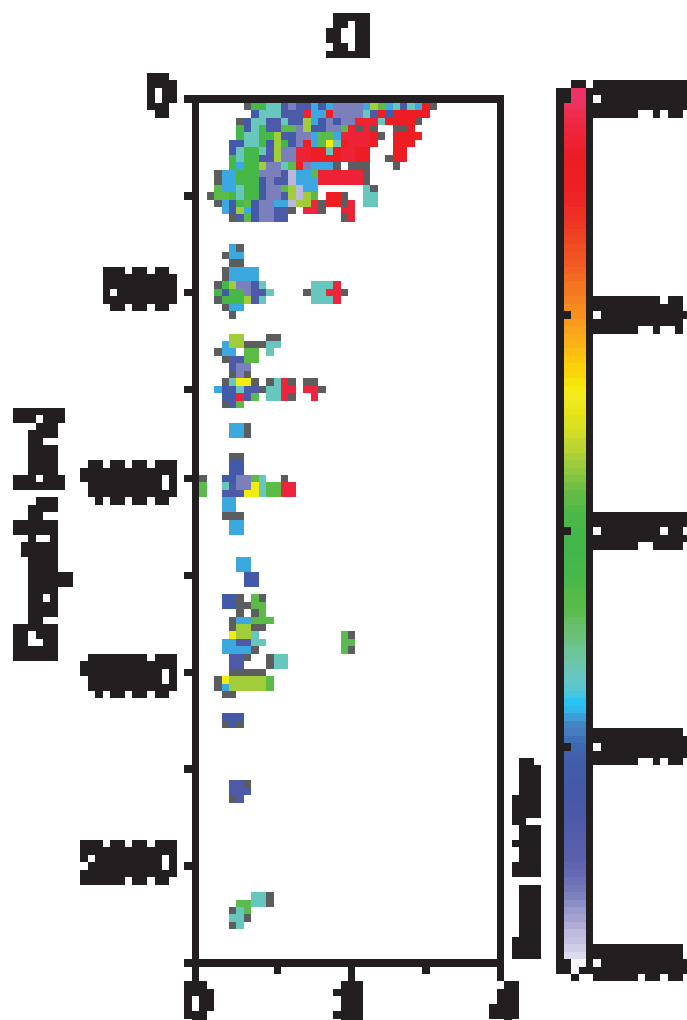


Figure 2: Aragonite saturation state (x-axis) at depth (m; y-axis) from the Seward Line in the GOA from spring (May) for 2008 to 2015. Red colors indicate most recent years influenced by the Blob. Data are preliminary.

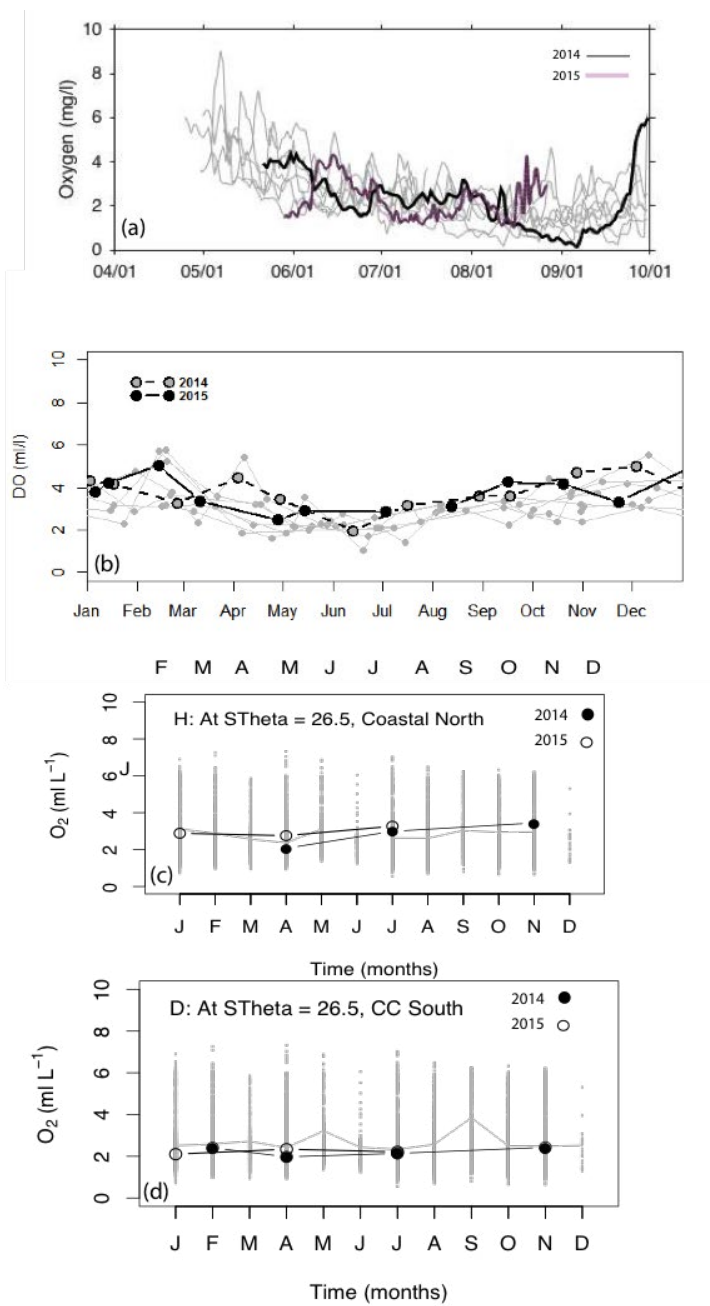


Figure 3: Oxygen concentrations from (a) a bottom mooring in Washington (Olympic Coast National Marine Sanctuary, station CEO42, 42 m depth, 2006-2015), (b) water samples from California, Trinidad Head Line (station TH02, 75 m depth, 2006-2015), and bottle samples at the 26.5 kg m⁻³ density level from the CALCOFI region in (c) coastal north and (d) California Current south. Grey lines on the upper two panels indicate data prior to 2014 (2006-2013). Grey dots on bottom two panels indicate averages from individual cruises from 1984-2013, while grey lines indicate climatological monthly averages over that period. Figures adapted from Leising et al. (2015).

Nitrate in the CCS

In 2014, nitrate concentrations in the surface waters found off of Newport, Oregon (NH-5 site, located in 60 m water depth) were anomalously low, especially during the upwelling season of spring/summer and even during fall when the Blob came onshore. Conditions reversed to anomalously high in 2015 with observations nearly 15 μM higher than the observed range in the early part of the upwelling season (Leising et al. 2015).

Chlorophyll in the CCS

In the spring of 2014 (March-May), before the Blob came onshore, chlorophyll was anomalously low in most regions along the West Coast. By the spring of 2015, chlorophyll was anomalously high over most of the CCS, but by later in the summer (July), chlorophyll returned to anomalously low conditions (Leising et al. 2015; Figure 4). These satellite-based results are consistent with in situ observations from Trinidad Head and the CALCOFI region for both years. Monterey Bay experienced higher than average chlorophyll conditions at the surface in 2014 and subsurface (~100 m) in 2015.

Massive blooms of phytoplankton were observed in situ in 2015 off of Newport, Oregon. Three harmful algal bloom species (primarily *Pseudo-nitzschia* and *Alexandrium* but also some *Akashiwo sanguinea*) created a large bloom event that resulted in elevated concentrations of domoic acid (a deadly neurotoxin that can cause paralytic shellfish poisoning) and saxitoxins (amnesic shellfish poisoning; Peterson et al. 2015)—which accumulated in the water column, sediments, and, ultimately, the marine food web. As a result, Oregon and Washington states closed the harvest of razor clams, mussels, and Dungeness crabs. The *Pseudo-nitzschia*

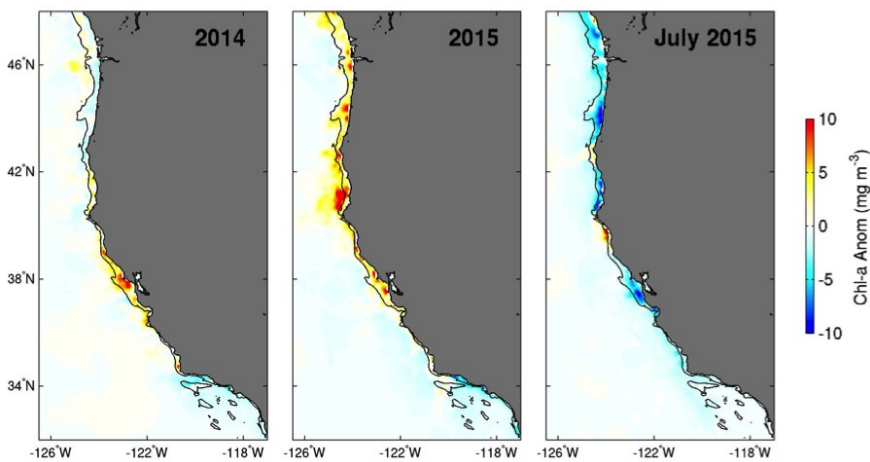


Figure 4: Chlorophyll a anomalies (mg m^{-3}) from Aqua MODIS in spring (March-May) of 2014 (left), spring (March-May) of 2015 (center), and July 2015 (right). Figure from Leising et al. (2015).

bloom extended all along the west coast up to the Gulf of Alaska, was considered one of the largest harmful algal bloom events in history, and resulted in the closure of the economically important Dungeness crab fishery.

Higher trophic level impacts in the CCS

A total of 17 new copepod species, having sub-tropical and tropical affinities, were found on the shelf and slope waters off Newport, Oregon, and are records for the NCC (northern California Current; Peterson et al. 2015). The copepod species richness at Newport indicates that the water that came ashore, associated now with the Blob at Newport (44.6°N), in autumn 2014 was from an offshore and southerly source (Peterson et al. 2015). High abundance of jellies were also observed off of coastal Oregon in 2015. Similar patterns were reported for copepods off northern California and gelatinous taxa off much of California (Leising et al. 2015).

Eggs of both sardines and anchovies were found in net tows off Newport in February and March of 2015, which was a "first" for the Oregon coast as these species usually spawn off southern California in late winter/early spring or in the NCC in summer (Peterson et al. 2015). Rockfish early life history stages experienced the lowest

abundance in Oregon over the previous four years, and flatfish was at its highest (Leising et al. 2015). Younger salmon populations were found to be low off of the NCC, while adult populations were mid-range to average. Warm years are expected to reduce the numbers of returning adults, and in the summer of 2015, the coho salmon returns in the Columbia River were the lowest in at least 25 years (Peterson et al. 2016).

Off northern and central California, pelagic communities associated with southern or offshore conditions were found together, which is unusual, and the region experienced abundant catches of juvenile rockfishes, which are commonly associated with cool-water conditions (Leising et al. 2015). Northward shifts of squid, sardine, and anchovy from southern California were observed, in conjunction with the arrival of southern species associated with El Niño conditions, including a rare occurrence of Dorado eggs off of Southern California, well north of their normal spawning grounds off of Mexico (Leising et al. 2015).

Peterson et al. (2015) reported observations of the presence of tropical seabirds in the NCC. In addition, two seabird mortality events occurred involving thousands of the local Cassin's Auklet off the Farallon Islands on November 16, 2014 and off the northern Oregon coast on December 22, 2014. Cassin's Auklet is a tiny seabird that dives to depths of 50 m in search of krill. Peterson et al. (2015) suggest that the birds likely perished because they could not penetrate the thick (~50-100 m) buoyant layer of warm waters to the cooler waters beneath that might have contained krill. However, the seabird species richness index reported for the CalCOFI region indicated near neutral conditions for Auklets in 2015—meaning their numbers were back to a normal range after the large mortality event. In 2014, sea lions experienced decreased weights and growth rates, and that trend continued in 2015 with large mortality events in California (Leising et al. 2015).

Lasting impacts?

In summary, the Blob had major effects beyond just temperature. In the open ocean, the Blob could have altered some portions of the Central Pacific from a sink to a source for carbon to the atmosphere. In coastal regions, the Blob brought warm, high oxygen, low carbon water to the CCS and the GOA. Ecosystems shifted northwards from the equatorial regions and harmful algae dominated the massive plankton bloom that erupted on the coast. The source of the nutrients that fueled that plankton bloom is the subject of current

research. While observations of high nutrients on the shelf were made in 2015, these results are inconsistent with the oxygen and carbon signals.

As the 2015-16 El Niño began to influence the Pacific, the Blob's influence was reduced (see Amaya et al., this issue). It is not clear, yet, whether the ocean biogeochemistry and ecosystem will also return to a relatively more "normal" state or if the Blob's impacts will continue to influence the Pacific post mortem. Only time and observations will tell.

References

- Bond, N. A., M. F. Cronin, H. Freeland, and N. Mantua, 2015: Causes and impacts of the 2014 warm anomaly in the Pacific. *Geophys. Res. Lett.*, **42**, 3414–3420, doi:[10.1002/2015GL063306](https://doi.org/10.1002/2015GL063306).
- Cosca, C. E., R. A. Feely, S.R . Alin, 2016: Data management and preservation of underway pCO₂ observations from VOS ships. ASLO Ocean Sciences Meeting, 2016 New Orleans.
- Feely, R. A., C. L. Sabine, J. M. Hernandez-Ayon, D. Ianson, and B. Hales, 2008: Evidence for upwelling of corrosive "acidified" water onto the continental shelf. *Science*, **320**, doi:[10.1126/science.1155676](https://doi.org/10.1126/science.1155676).
- Leising, A. W., and Coauthors, 2015: State of the California Current 2014-15: Impacts of the warm-water "Blob." CalCOFI Rep., **56**, 31-68, <http://www.calcofi.org/publications/calcofireports/v56/Vol56-SOTCC.web.31-69.pdf>.
- National Marine Fisheries Service, 2014: Fisheries economics of the United States, 2012. U.S. Dept. Commerce, NOAA Tech. Memo. NMFS-F/SPO-137, 175p., <https://www.st.nmfs.noaa.gov/st5/publication/index.html>.
- Peterson, W., M. Robert, and N. Bond, 2015: The warm blob continues to dominate the ecosystem of the northern California Current. PICES Press, **23**, 44-46, https://www.pices.int/publications/pices_press/volume23/PPJuly2015.pdf.
- Peterson, W., N. Bond and M. Robert, 2016: The Blob (Part Three): Going, going, gone?. PICES Press, **24**, 46-48, https://www.pices.int/publications/pices_press/volume24/PPJan2016.pdf.
- Waldbusser, G. G., B. Hales, C. J. Langdon, B. A. Haley, P. Scrader, E. L. Brunner, M. W. Gray, C. A. Miller, and I. Gimenez, 2015: Saturation-state sensitivity of marine bivalve larvae to ocean acidification, *Nat. Climate Change*, **5**, 273–280, doi:[10.1038/nclimate2479](https://doi.org/10.1038/nclimate2479).



Key dates for CLIVAR Open Science Conference

June 15

Early Bird Registration

Town Hall Submissions

Climate interpretation of the North Pacific marine heatwave of 2013-2015

Emanuele Di Lorenzo¹, Giovanni Liguori¹, and Nathan Mantua²

¹Georgia Institute of Technology

²National Marine Fisheries Service, NOAA

The prolonged and record-breaking warming of the Northeast Pacific Ocean between the winters of 2013/14 and 2014/15, also referred to as the “Warm Blob” or more generally as a marine heatwave (Hobday et al. 2016), had extreme impacts on marine ecosystems, some of which are ongoing ([see Siedlecki et al. this issue](#)). Whether these multi-year climate extremes will become more frequent under greenhouse forcing is a key question for scientists, resource managers, and society. Here we interpret the forcing, persistence, and evolution of the warm blob in the context of the large-scale climate dynamics of the Pacific Ocean. After identifying these dynamics, we explore the warm blob mechanisms in the Community Earth System Model Large Ensemble (CESM-LE) to quantify how and if the climate variance of the North Pacific is impacted by greenhouse forcing.

Relationship between the Warm Blob patterns and Pacific climate modes

It has been previously noted that the spatial pattern of the warm blob evolved in space and time from the winter of 2014 to the winter of 2015, here defined as the January–February–March (JFM) mean ([see Amaya et al. this issue](#)). While in JFM of 2014, the warm water mass is centered in the Gulf of Alaska (GOA), in the following winter of 2015 the warm waters spreads along the entire

Pacific coast of North America to form the so called ARC pattern. These two types of patterns are recurrent in the Northeast Pacific and captured by the two dominant modes of winter sea surface temperature anomalies (SSTA) inferred by an Empirical Orthogonal Function (EOF) analysis (Figure 1a and 1b). If we compare the timeseries of the winter SSTA values averaged in the center of the GOA pattern ([see Amaya et al. this issue](#)) with the timeseries of EOF2, referred to as the second Principal Components (PC2), we find a correlation of $R=0.95$ and a clear maximum in 2014 (Figure 1c). The same is true if we compare with EOF2/PC2 (Figure 1d). Both the GOA and ARC pattern that emerge in the wintertime SSTA EOFs are connected to well known modes of climate variability such as the North Pacific Gyre Oscillation (NPGO, Di Lorenzo et al. 2008) and the Pacific Decadal Oscillation (PDO, Mantua et al. 1997). Specifically, the GOA pattern is connected to NPGO-like variability ($R=0.71$, Figure 1c), while the ARC pattern tracks PDO-like variability ($R=0.75$, Figure 1d). The NPGO and PDO are ocean expressions of atmospheric forcing associated with changes in the North Pacific Oscillation (NPO) and in the strength and location of the Aleutian Low (AL; Di Lorenzo et al. 2008; Chhak et al., 2009). Consistent with this view, it has been shown that in 2014 the GOA pattern was forced by atmospheric variability typical of the NPO (Bond et al. 2015; Wang et al. 2014; Hartman 2015; Seager et al. 2015);

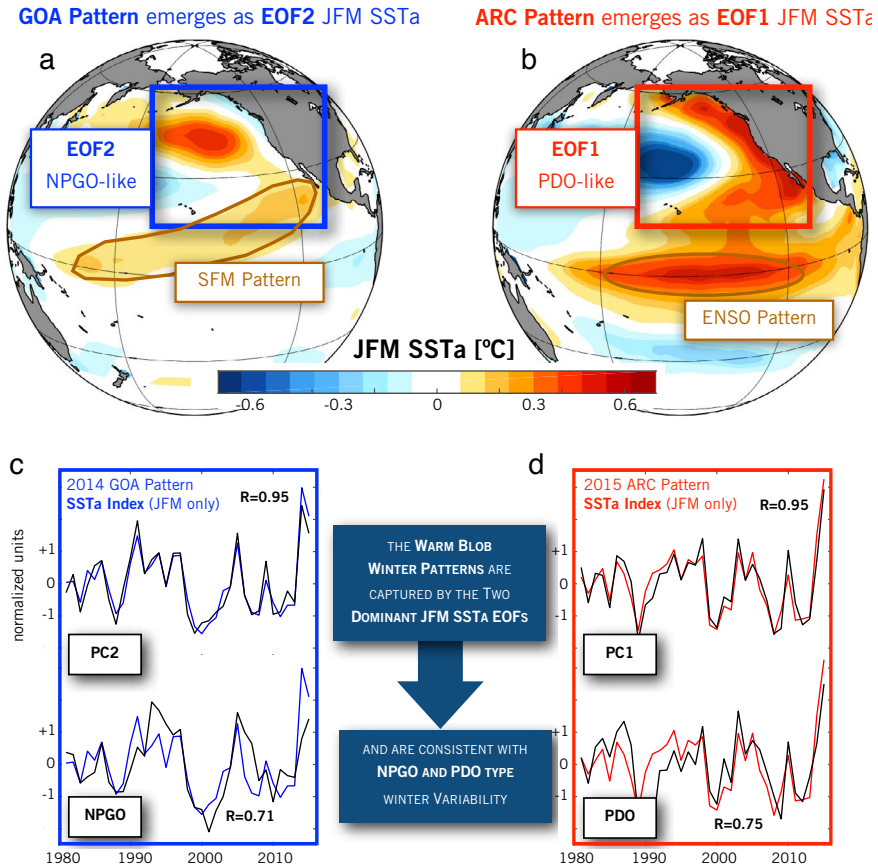


Figure 1: Relationship of Warm Blob Patterns to Dominant EOFs. Dominant patterns of winter (JFM) SSTa ($^{\circ}\text{C}$) variability in the Northeast Pacific inferred from Empirical Orthogonal Functions (EOFs; are computed over the region outlined by the blue and red bounding boxes, the principal components are then regressed on Pacific JFM SSTa). (a) EOF2 and (b) EOF1 capture the GOA and ARC patterns observed in the evolution of the Warm Blob from JFM 2014 to JFM 2015. (c) The timeseries of the GOA SSTa pattern are strongly correlated to PC2 and exhibit an NPGO-like variability. (d) The timeseries of the ARC SSTa pattern are strongly correlated to PC1 and exhibit an NPGO-like variability. EOF1 and EOF2 explain $\sim 60\%$ and $\sim 22\%$ of the winter SSTa variance. [Figure redrawn from Di Lorenzo and Mantua 2016]

Anderson et al. 2016; Baxter and Nigam 2015), while in 2015 a stronger AL forced the ARC pattern (Di Lorenzo and Mantua 2016). This result is recovered by a simple correlation of the JFM SSTa PC2 (GOA pattern) and PC1 (ARC pattern) with sea level pressure anomalies (SLPa; Figure 2a and 2b). The SLPa correlation patterns show the typical dipole structure of the NPO (Figure 2a) as the

forcing of the GOA pattern and a deeper AL (Figure 2b) as the forcing of the GOA pattern.

Climate mechanisms underlying the evolution and persistence of the Warm Blob

The close similarity of the ocean and atmosphere patterns of the warm blob in 2014 and 2015 with known modes of climate variability (e.g., NPO/NPGO in 2014, AL/PDO in 2015) allows us to use previous knowledge of large-scale Pacific climate dynamics to interpret the forcing, evolution, and persistence of the blob. In 2014, the winter NPO-like atmospheric forcing of the GOA SSTa pattern (Figure 2a) is connected to well-known El Niño precursor dynamics referred to as the seasonal footprinting mechanisms (SFM, Vimont et al. 2003). Specifically, the subtropical expression of the NPO (e.g., around Hawaii, SFM region in Figure 2a) causes a reduction of the trade winds, which in turn reduces evaporation and generates warm SSTa, as evident in the JFM SSTa EOF2 (Figure 1a, SFM region). This coupling between the ocean and atmosphere creates a positive feedback between winds-evaporation-SST (Xie et al. 1999), which energizes the so-called “meridional modes” (Chiang and Vimont 2004; Vimont 2010). The

meridional modes propagate and amplify the SSTa in the spring from the subtropics into the central equatorial Pacific. Once these positive SSTa arrive at the equator, they favor the development of the El Niño Southern Oscillation (ENSO) (Alexander et al. 2010). Once El Niño variability begins to peak in the fall, the re-arrangement of tropical convection excites atmospheric ENSO

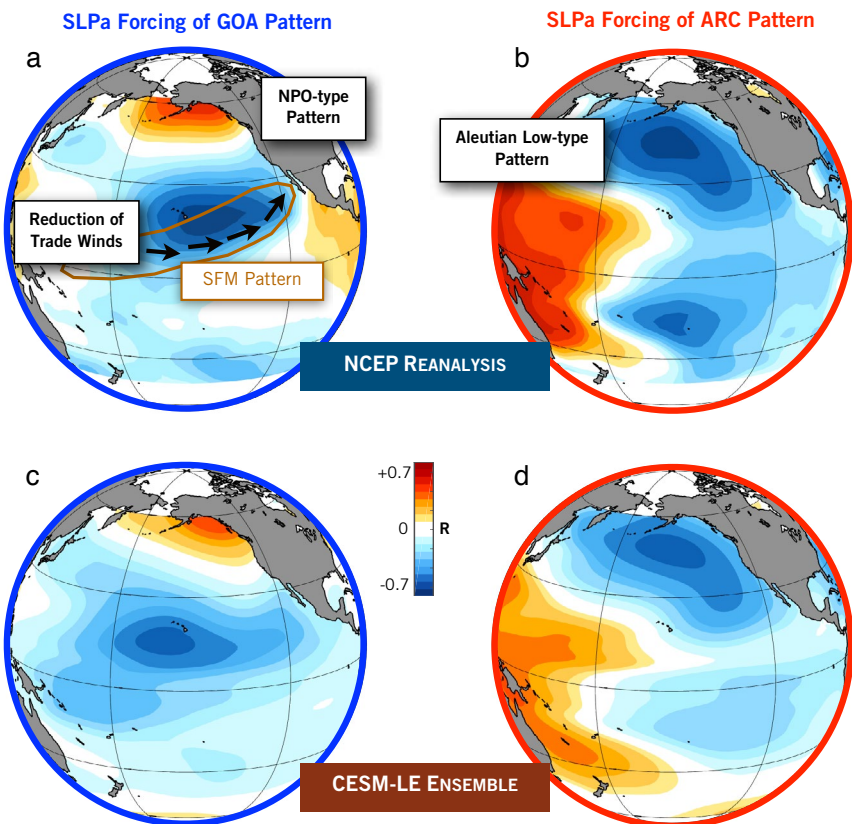


Figure 2: Atmospheric Forcing of Warm Blob Patterns. Correlation of JFM SSTa PCs in the Northeast Pacific with SLPa. PC2 and PC1 track the GOA (a) and ARC (b) patterns in the SSTa and are used to extract the corresponding patterns of atmospheric forcing. The same analysis is conducted on the Community Earth System Model Large Ensemble (CESM-LE, 30 members). The ensemble mean patterns are shown in (c) for CESM-LE PC2 and in (d) for CESM-LE PC1.

teleconnections that inject variance into the extratropical atmosphere, which ultimately impacts the AL variability in the next boreal winter (Alexander et al. 2002). It is the changes in the AL that drive the oceanic PDO-type expression in winter SSTa (Figure 1b; Newman et al. 2003; Schneider and Cornuelle 2005). This succession of events, which is summarized in Figure 3 in the context of the 2014/15 warm blob evolution (Steps 1, 2, 3, and 4), is shown to be an important source of the persistence and reinforcement of the blob ARC pattern in the winter of 2015 (Di Lorenzo and Mantua 2016). Although the El Niño expression in the fall of 2014 (Figure 3) appears

weak, the ENSO teleconnections still account for ~50% of the ARC warming pattern of 2015 (Di Lorenzo and Mantua 2016). Other research also strongly suggests that teleconnections from the tropics to the extratropics contributed to the exceptional persistence of the NPO-type variability in 2014 (Hartmann 2015; Seager et al. 2015). These teleconnection dynamics, from extratropics (winter year 0) to tropics to extratropics (winter year +1), have been shown to be important mechanisms and memory for generating Pacific decadal and multi-decadal variability (Di Lorenzo et al. 2015), and are here recognized as potential mechanisms for the multi-year persistence and evolution of SSTa ocean extremes in the Northeast Pacific.

Changes in variance of the Warm Blob patterns under greenhouse forcing

Previous studies have suggested that the NPO-type variability that initiated the drought in 2014 will intensify in response to greenhouse forcing (Wang et al. 2015; 2015; Yoon et al. 2015; Sydeman et al. 2013). This

suggests that the oceanic expression of the NPO, that is the GOA/NPGO-like pattern, will also increase in variance. Unfortunately current observations are not sufficient to test if the North Pacific variance has increased. In fact, Johnstone and Mantua (2014) suggest that observed SST variations and trends in the Northeast Pacific from 1900–2012 are largely a response to atmospheric forcing that shows no robust century-scale trends in CMIP5 historical forcing experiments and that instead may be one phase in the slow (~10 year) progression of atmospheric pressures around the North Pacific (Anderson et al. 2016).

CLIMATE INTERPRETATION for the WARM BLOB of 2014/15

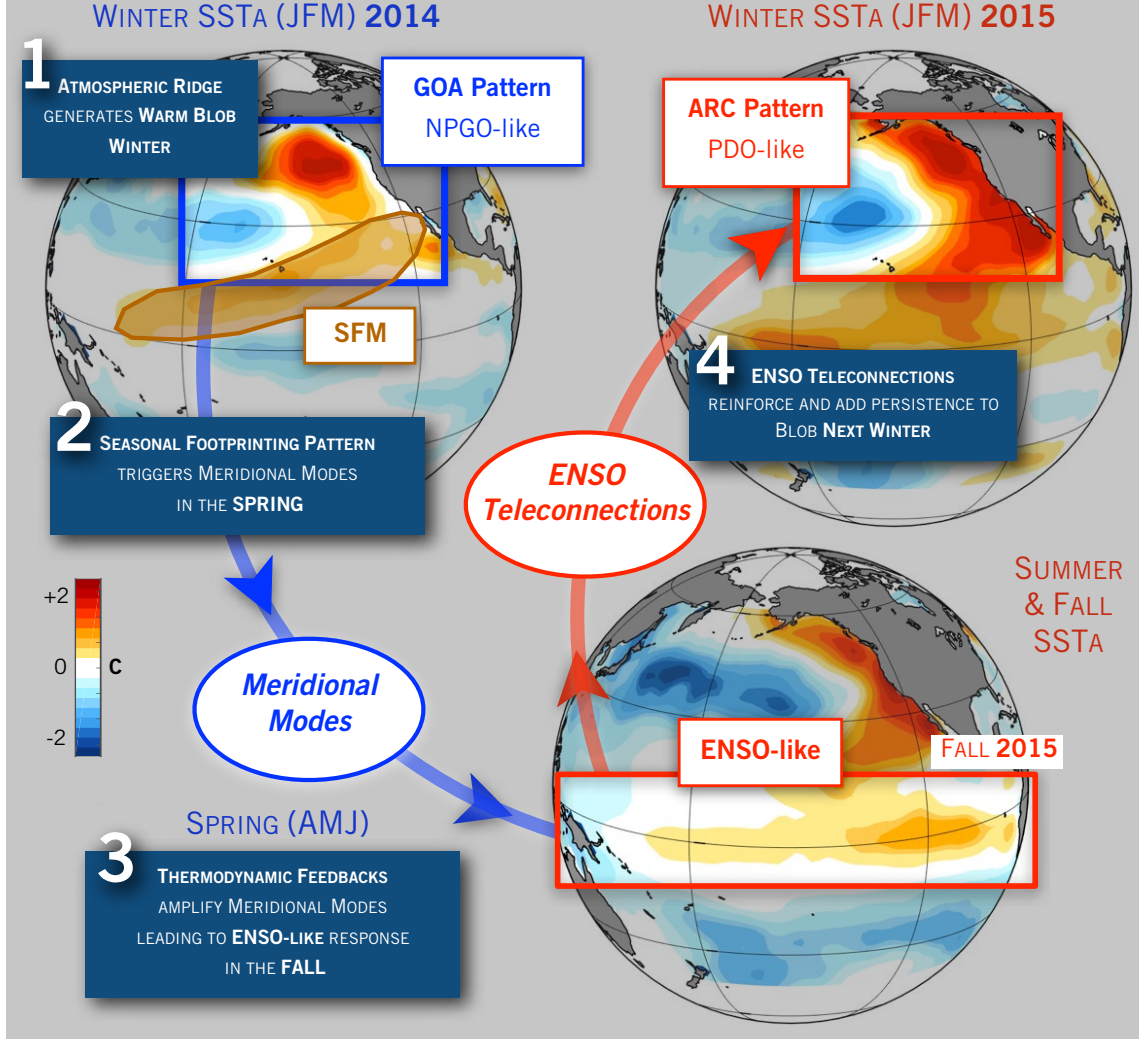


Figure 3: Schematic of SSTa ($^{\circ}\text{C}$) evolution associated with the warm blob from the winter of 2014 to winter of 2015 and relationship to mechanisms of large-scale climate variability.

To better separate the changes in North Pacific SSTa variance that are internal (e.g., natural) from the forced (e.g., climate change), we explore the variability of the GOA and ARC winter patterns in the Community Earth System Model Large Ensemble (CESM-LE greenhouse simulations, 30 ensemble members from 1920-2100 under the regional concentration pathway (RCP8.5)

scenario (Kay et al. 2015). We extract the GOA and ARC pattern with the same approach used for the observations by computing the EOF1 and EOF2 of the JFM SSTa over the Northeast Pacific region (Figure 4a and 4b). The EOFs are computed for each of the 30 ensemble members, and then the patterns are averaged together to obtain an ensemble mean EOF structure. The CESM-LE EOFs are

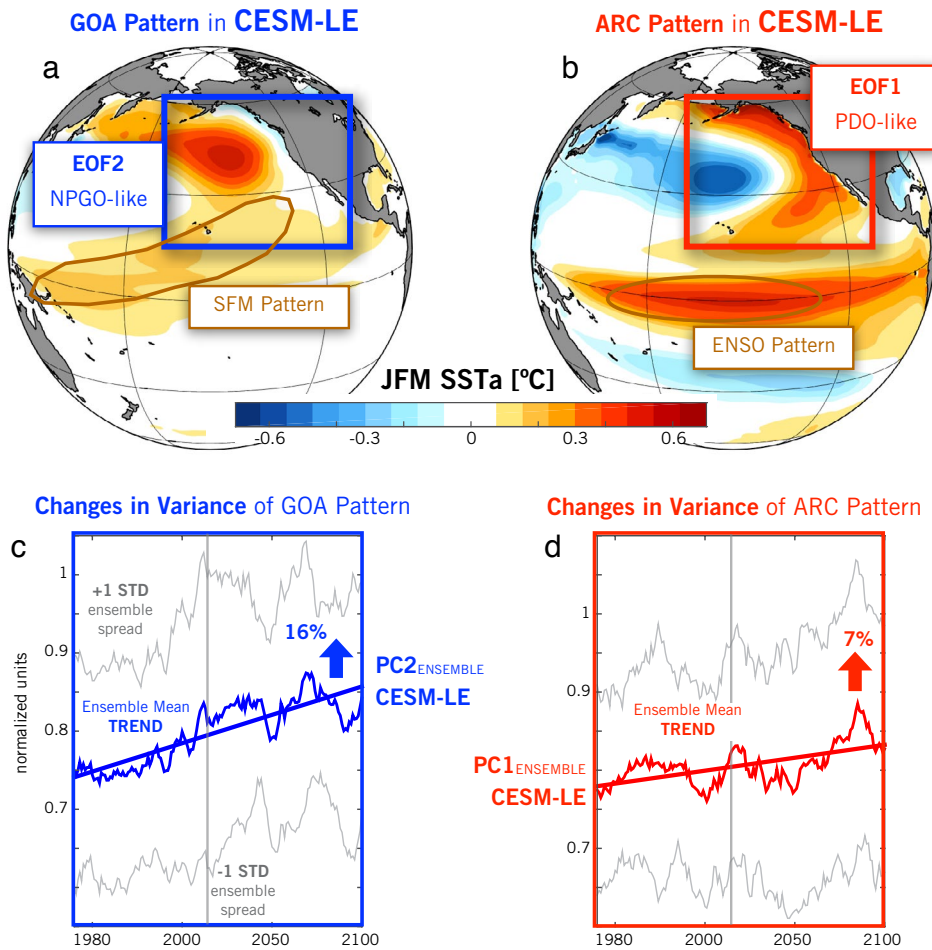


Figure 4: Warm Blob JFM Patterns under Greenhouse forcing. Dominant patterns of winter (JFM) SST_a (°C) variability in the Northeast Pacific from the CESM-LE (blue and red bounding boxes) inferred the two dominant EOFs from 1920-2100 under the RCP8.5 greenhouse scenario. (a) EOF2 and (b) EOF1 capture the warm blob GOA and ARC patterns. The SFM and ENSO pattern in the CESM-LE are shifted to the west, a known bias of climate models. The 20-year running variance of the PCs show an increase in variance. (c) The PC2 shows an increase of 16% in the variance of the GOA SST_a pattern, while PC1 an increase in 7% of the ARC pattern. EOF1 and EOF2 explains ~67% and ~22% of the winter SST_a variance. [Figure redrawn from Di Lorenzo and Mantua 2016]

almost identical to the observations (compare with Figure 1a and 1b) and explain a similar amount of variance. Given the close similarity between the observations and the model simulations, we quantify the anthropogenically forced changes in the variance of the GOA and ARC patterns by computing the 20-year running variance of the CESM-LE PC2 and PC1. The ensemble mean of the running variance shows a significant trend in the GOA

pattern (PC1) with an increase of ~16% from 1920 to 2100 (Figure 4c). The variance of the ARC pattern also increases but only by ~7% (Figure 4d). Given that the forcing pattern of the GOA pattern (EOF2) in the CESM-LE also captures the typical NPO structure (Figure 2c), there is strong indication that the NPO/NPGO-like variability associated with the GOA pattern may intensify under greenhouse forcing (see also Sydeman et al. 2013 for an observational analysis).

The intensification of the NPO activity is likely linked to the activity of meridional modes. Preliminary analysis of the CESM-LE (Liguorietal., personal communication) reveals that the thermodynamic coupling between ocean and atmosphere associated with the winds-evaporation-SST feedback is intensifying. This may lead not only to an enhanced variance of the NPO system, but to a stronger coupling between meridional modes and ENSO. This stronger coupling results from the propagation of larger

amplitude meridional modes SST anomalies from the subtropics to the tropics, where they are more likely to trigger ENSO and its teleconnections back to the extratropics (e.g., multi-year memory). An intensification of the meridional modes/ENSO coupling should translate into a stronger coupling between the GOA pattern and the following year ARC pattern (e.g., multi-year warm events).

While the analyses and discussion presented in this short article lay out a set of mechanistic pathways/hypotheses to understand warm blob dynamics and the climate teleconnections that lead to multi-year persistence of

ocean SSTa extremes in the Northeast Pacific, future studies will need to develop numerical experiments to test these dynamics under the uncertainties of a changing climate with a large range of natural decadal variability.

References

- Alexander, M. A., I. Blade, M. Newman, J. R. Lanzante, N. C. Lau, and J. D. Scott, 2002: The atmospheric bridge: The influence of ENSO teleconnections on air-sea interaction over the global oceans. *J. Climate*, **15**, 2205-2231, doi:[10.1175/1520-0442\(2002\)015<2205:btio>2.0.co;2](https://doi.org/10.1175/1520-0442(2002)015<2205:btio>2.0.co;2).
- Alexander, M. A., D. J. Vimont, P. Chang, and J. D. Scott, 2010: The impact of extratropical atmospheric variability on ENSO: Testing the seasonal footprinting mechanism using coupled model experiments. *J. Climate*, **23**, 2885-2901, doi:[10.1175/2010jcli3205.1](https://doi.org/10.1175/2010jcli3205.1).
- Anderson, B. T., D. J. Gianotti, J. C. Furtado, and E. Di Lorenzo, 2016: A decadal precession of atmospheric pressures over the North Pacific. *Geophys. Res. Lett.*, **43**, doi:[10.1002/2016GL068206](https://doi.org/10.1002/2016GL068206).
- Baxter, S., and S. Nigam (2015), Key Role of the North Pacific Oscillation-West Pacific Pattern in Generating the Extreme 2013/14 North American Winter, *J. Climate*, **28** (20), 8109-8117, doi:[10.1175/jcli-d-14-00726.1](https://doi.org/10.1175/jcli-d-14-00726.1).
- Bond, N. A., M. F. Cronin, H. Freeland, and N. Mantua, 2015: Causes and impacts of the 2014 warm anomaly in the NE Pacific. *Geophys. Res. Lett.*, **42**, 3414-3420, doi:[10.1002/2015gl063306](https://doi.org/10.1002/2015gl063306).
- Chhak, K. C., E. Di Lorenzo, N. Schneider, and P. F. Cummins, 2009: Forcing of low-frequency ocean variability in the Northeast Pacific. *J. Climate*, **22**, 1255-1276, doi:[10.1175/2008jcli2639.1](https://doi.org/10.1175/2008jcli2639.1).
- Chiang, J. C. H., and D. J. Vimont, 2004: Analogous Pacific and Atlantic meridional modes of tropical atmosphere-ocean variability. *J. Climate*, **17**, 4143-4158, doi:[10.1175/jcli4953.1](https://doi.org/10.1175/jcli4953.1).
- Di Lorenzo, E. and N. Mantua, 2016: Multi-year persistence of the 2014/15 North Pacific marine heatwave. *Nat. Climate Change*, accepted.
- Di Lorenzo, E., and Coauthors, 2008: North Pacific Gyre Oscillation links ocean climate and ecosystem change. *Geophys. Res. Lett.*, **35**, doi:[10.1029/2007gl032838](https://doi.org/10.1029/2007gl032838).
- Di Lorenzo, E., G. Liguori, J. Furtado, N. Schneider, B. T. Anderson, and M. Alexander, 2015: ENSO and meridional modes: a null hypothesis for Pacific climate variability. *Geophys. Res. Lett.*, **42**, doi:[10.1002/2015gl066281](https://doi.org/10.1002/2015gl066281).
- Hartmann, D. L., 2015: Pacific sea surface temperature and the winter of 2014. *Geophys. Res. Lett.*, **42**, 1894-1902, doi:[10.1002/2015gl063083](https://doi.org/10.1002/2015gl063083).
- Hobday, A. J., and Coauthors, 2016: A hierarchical approach to defining marine heatwaves. *Prog. Oceanogr.*, **141**, 227-236, doi:[10.1016/j.pocean.2015.12.014](https://doi.org/10.1016/j.pocean.2015.12.014).
- Johnstone, J. A., and N. J. Mantua, 2014: Atmospheric controls on northeast Pacific temperature trends and variations, 1900-2012. *Proc. Nat. Acad. Sci.*, **111**, 14360-14365, doi:[10.1073/pnas.1318371111](https://doi.org/10.1073/pnas.1318371111).
- Kay, J. E., and Coauthors, 2015: The Community Earth System Model (CESM) Large Ensemble Project: A community resource for studying climate change in the presence of internal climate variability. *Bull. Amer. Meteorol. Soc.*, **96**, 1333-1349 doi:[10.1175/BAMS-D-13-00255.1](https://doi.org/10.1175/BAMS-D-13-00255.1).
- Mantua, N. J., S. R. Hare, Y. Zhang, J. M. Wallace, and R. C. Francis, 1997: A Pacific interdecadal climate oscillation with impacts on salmon production. *Bull. Amer. Meteorol. Soc.*, **78**, 1069-1079, doi:[10.1175/1520-0477](https://doi.org/10.1175/1520-0477).
- Newman, M., G. P. Compo, and M. A. Alexander, 2003: ENSO-forced variability of the Pacific Decadal Oscillation. *J. Climate*, **16**, 3853-3857, doi:[10.1175/1520-0442](https://doi.org/10.1175/1520-0442).
- Schneider, N., and B. D. Cornuelle, 2005: The forcing of the Pacific Decadal Oscillation. *J. Climate*, **18**, 4355-4373, doi:[10.1175/jcli3527.1](https://doi.org/10.1175/jcli3527.1).
- Seager, R., M. Hoerling, S. Schubert, H. L. Wang, B. Lyon, A. Kumar, J. Nakamura, and N. Henderson, 2015: Causes of the 2011-14 California drought*. *J. Climate*, **28**, 6997-7024, doi:[10.1175/jcli-d-14-00860.1](https://doi.org/10.1175/jcli-d-14-00860.1).
- Sydeman, W. J., J. A. Santora, S. A. Thompson, B. Marinovic, and E. Di Lorenzo, 2013: Increasing variance in North Pacific climate relates to unprecedented ecosystem variability off California. *Global Change Bio.*, **19**, 1662-1675, doi:[10.1111/gcb.12165](https://doi.org/10.1111/gcb.12165).
- Vimont, D. J., 2010: Transient growth of thermodynamically coupled variations in the tropics under an equatorially symmetric mean. *J. Climate*, **23**, 5771-5789, doi:[10.1175/2010jcli3532.1](https://doi.org/10.1175/2010jcli3532.1).
- Vimont, D. J., J. M. Wallace, and D. S. Battisti, 2003: The seasonal footprinting mechanism in the Pacific: Implications for ENSO. *J. Climate*, **16**, 2668-2675, doi:[10.1175/1520-0442\(2003\)016<2668:tsfmit>2.0.co;2](https://doi.org/10.1175/1520-0442(2003)016<2668:tsfmit>2.0.co;2).
- Wang, S. Y., L. Hipps, R. R. Gillies, and J. H. Yoon, 2014: Probable causes of the abnormal ridge accompanying the 2013-2014 California drought: ENSO precursor and anthropogenic warming footprint. *Geophys. Res. Lett.*, **41**, 3220-3226, doi:[10.1002/2014gl059748](https://doi.org/10.1002/2014gl059748).
- Wang, S. Y. S., W. R. Huang, and J. H. Yoon, 2015: The North American winter 'dipole' and extremes activity: a CMIP5 assessment. *Atmos. Sci. Lett.*, **16**, 338-345, doi:[10.1002/asl2.565](https://doi.org/10.1002/asl2.565).
- Xie, S. P., 1999: A dynamic ocean-atmosphere model of the tropical Atlantic decadal variability. *J. Climate*, **12**, 64-70, doi:[10.1175/1520-0442-12.1.64](https://doi.org/10.1175/1520-0442-12.1.64).
- Yoon, J. H., S. Y. S. Wang, R. R. Gillies, B. Kravitz, L. Hipps, and P. J. Rasch, 2015: Increasing water cycle extremes in California in relation to ENSO cycle under global warming. *Nat. Commun.*, **6**, doi:[10.1038/ncomms9657](https://doi.org/10.1038/ncomms9657).

The tale of a surprisingly cold blob in the North Atlantic

Aurélie DUCHEZ¹, Damien DESBRUYÈRES¹, Joël J.-M. HIRSCHI¹, Eleanor Frajka-Williams², Simon JOSEY¹, and Dafydd GWYN EVAN²

¹National Oceanography Centre Southampton, UK

²University of Southampton, UK

Climate change is usually assessed over years and decades, and 2015 shattered the record set in 2014 for the hottest year yet recorded for the globe's surface land and oceans since 1850. The year 2016 is also expected to set a new record, with the average global surface temperature in February 1.35°C warmer than the average temperature for the month between 1951-1980, a far bigger margin than ever seen before ([see NASA Earth Observatory](#)). Yet, one part of the planet is bucking the global sea surface temperature (SST) and upper ocean heat content (OHC) trends: southeast of Greenland and Iceland, the ocean surface has seen record cold temperatures for the past eight months of 2015.

The SST anomaly field for June 2015 (Figure 1a; 2a) shows temperatures up to 2°C colder than the 1948-2015 average. The coldest values observed over the central North Atlantic between 45°N and 60°N for this month of the year (indicated by stippling) encompass much of the eastern Subpolar Gyre. This cold "blob" represents a striking acceleration of a decadal drop in OHC that started in 2005 (Figure 1b). This negative trend may be marking a transition toward a new cold phase of the subpolar North Atlantic, following a persistent period of anomalously warm upper waters (1995-2014). The sharply cold feature reaches down to about 700 m depth, and opposes a warming trend in the intermediate layer (700 m - 2000 m) observed since the early 2000s (Figure

1d). The result is a cold anomaly in the surface layer, and increased stratification below.

Duchez et al. (2016) recently investigated the origin of the 2015 North Atlantic cold blob using reanalyses of observational data. As described below, a combination of air-sea heat loss from late 2014 through to spring 2015 and a re-emergent 2014 sub-surface OHC anomaly stand as the primary sources of the blob. The authors show that this cold Atlantic anomaly observed since 2014 is likely due to processes acting on sub-annual timescales. Consequently, this blob should not be confused with the long-term warming hole (located to the south-west of the 2015 anomaly) described by Rahmstorf et al. (2015) and Drijfhout et al. (2012) using numerical ocean models, which was identified on interannual and longer timescales. The long-term cold anomaly is presumably driven by a longer-term slowdown of the Atlantic Meridional Overturning Circulation (AMOC) and the associated reduction in northward oceanic heat transport. It is noteworthy that a 10-year long decline of the AMOC has been observed at 26°N by the RAPID array which has been monitoring the AMOC since 2004 (Smeed et al. 2014). Both the long-term trend as well as the seasonal to interannual variability of the AMOC can potentially impact the North Atlantic temperature (Duchez et al. 2015, Bryden et al. 2014).

Previous model and observation based studies suggest that atmospheric circulation changes can develop in

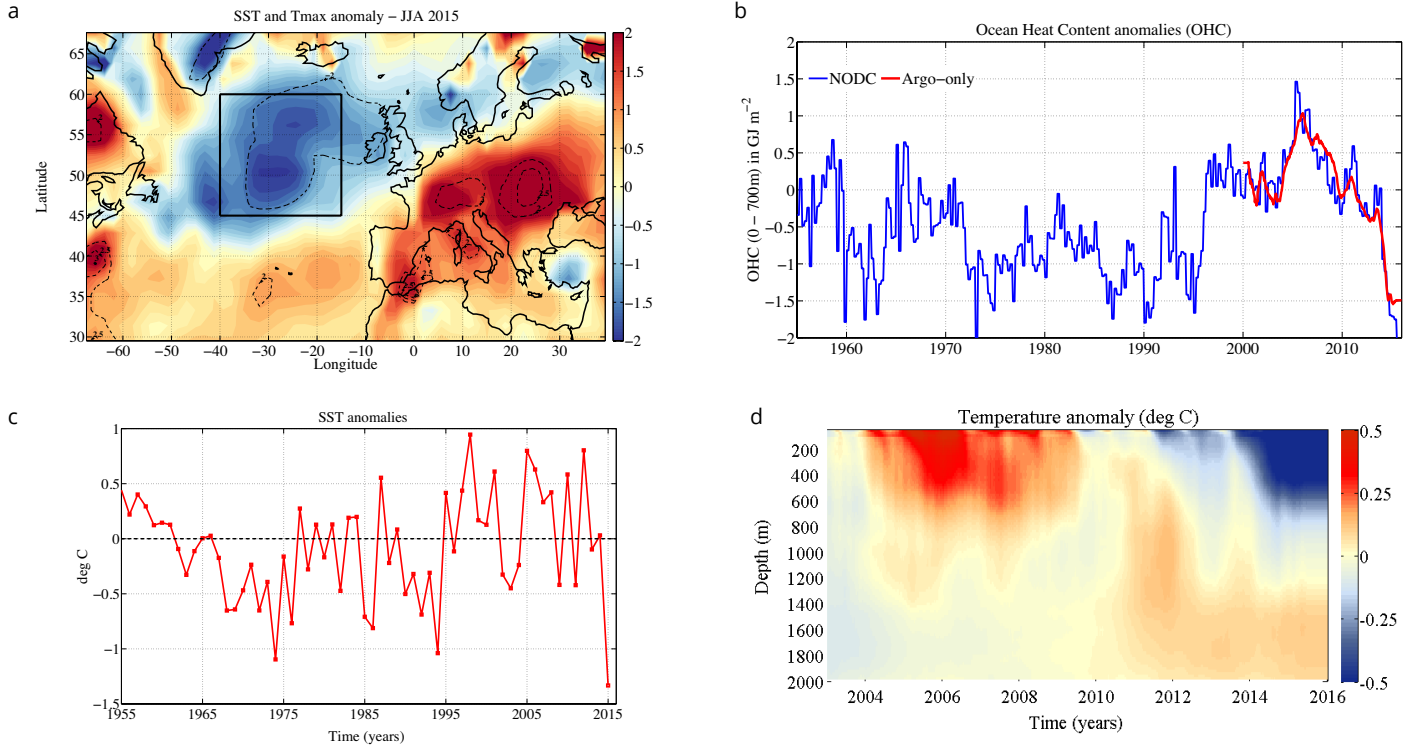


Figure 1: (a) June-August (JJA) 2015 SST anomalies (over the ocean) and maximum 2 m air temperature anomalies (over land) in °C (shading). Contours delineate regions exceeding 2 and 2.5 standard deviations. The box indicates the area chosen to define the cold Atlantic SST anomaly. (b) OHC anomaly timeseries up to December 2015 averaged over the box (45–60°N, 40–15°W) and extracted from the National Oceanographic Data Center (NODC) 0–700 m product (blue). Argo profiles represent the main source of data after 2003, as shown by an Argo-only index smoothed with a 12-month running window (red). Both timeseries are referenced to the period 2000–2015. (c) Timeseries of SST anomaly over the box shown on panel (a). (d) Time-depth diagram of the temperature anomaly in the subpolar box.

response to SST anomalies (Walsh 1982, Sutton and Mathieu 2002, Nakamura et al. 2005, Black and Sutton 2007, Buchan et al. 2014). Following the development of the 2015 cold ocean anomaly, Central Europe experienced a major summer heat wave that has been ranked in the top ten over the past 65 years (Russo et al. 2015, Ducez et al. 2016). The high temperatures coincided with persistent high and low-pressure systems over Europe and the central North Atlantic respectively, which subjected Central Europe to the influence of subtropical air masses. A causal relationship between the 2015 Atlantic cold blob and the subsequent European heat wave is hence highly plausible, and regional climate predictability will greatly benefit from the understanding of the driving mechanisms.

Origins of the Blob

Variations in SST are governed through the heat balance in the surface mixed layer of the ocean, which is influenced by surface air-sea heat fluxes (driven by wind speed, air temperature, cloudiness, and humidity), horizontal advective and diffusive processes in the mixed layer, and entrainment processes at the base of the mixed layer. In order to fully explain the origins of the cold ocean anomaly, we assess the respective contribution of surface air-sea fluxes, ocean circulation changes, and vertical water motion through Ekman upwelling.

A cold SST anomaly, with peak values at approximately 50°N, 30°W (Figure 2c), was apparent in observations

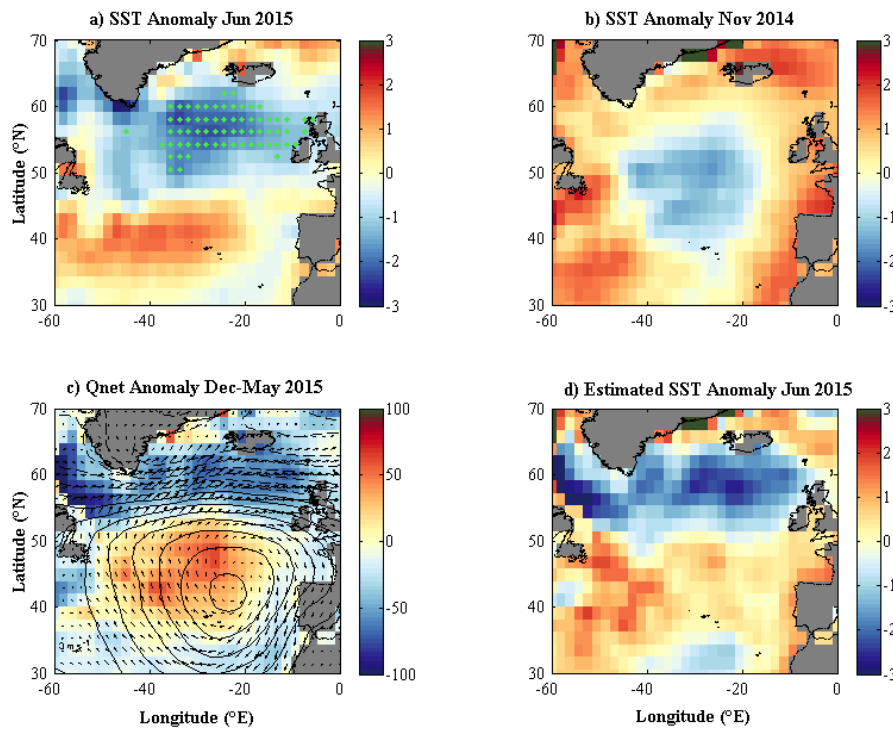


Figure 2: (a) June 2015 observed SST anomaly ($^{\circ}\text{C}$), stippled green cells show where the SST is the coldest for June in the period 1948-2015; (b) November 2014 observed SST anomaly ($^{\circ}\text{C}$); (c) December 2014-May 2015 averaged net heat flux (colored field in W m^{-2}) with corresponding SLP anomaly (contoured, 1 mb intervals, negative contours dashed) and 10 m wind speed anomaly (arrows), (d) June 2015 estimated SST anomaly ($^{\circ}\text{C}$) obtained by integrating the heat flux anomaly in (c) over the ocean mixed layer and adding to the November 2014 initial state in (b). All fields are from the NCEP/NCAR reanalysis.

made before the 2014/15 winter. This feature is consistent with a re-emergent cold, subsurface anomaly that was driven by extreme surface heat loss in winter 2013/14 (Grist et al. 2015). In the subsequent winter 2014/15, further extreme heat loss was observed but displaced northwards from that seen in 2013/14. The 2014/15 heat loss is associated with a prolonged positive state of the North Atlantic Oscillation (NAO, mean index of 1.03 using Climate Prediction Center mode values), which is characterised by stronger westerly winds resulting from an intensification of the meridional surface pressure gradient. Consequently, the subpolar North Atlantic (55-65°N) experienced severe heat loss to the atmosphere. We have estimated whether this heat loss

can account for the cold blob in June 2015 by calculating the SST anomaly expected by applying the December 2014-May 2015 surface heat flux anomaly to an ocean mixed layer of 100 m depth (close to the mean mixed layer depth (MLD) for the box in Figure 1a). The resulting heat flux implied anomaly is added to the initial November 2014 SST field (see Ducharé et al. 2016 for the method). The estimated field (Figure 2d) exhibits the main features of the observed subtropical-subpolar SST dipole (Figure 2a), with the best agreement being found in the eastern subpolar gyre. Thus, the effects of severe 2014/15 winter surface heat loss combined with the pre-existing re-emergent SST anomaly in November 2014 account for the cold blob.

From 2013 to 2015, the observed cooling of the 0-700 m layer between 45-60°N, 40-15°W represents an OHC change of 0.9 GJ m^{-2} , with two thirds (0.6 GJ m^{-2}) of this change occurring between December 2013 and January 2014 (Figure 1b). Such a change can either occur through a transformation of water masses by air-sea heat fluxes, or via a net increase in the lateral input of water into colder temperature classes. In fact, the relatively short timescales involved here also suggest that part of the cooling may result from wind-driven heave (adiabatic upwelling or downwelling of water masses). To quantify this potential effect, we select the volume of water above the 27.6 kg m^{-3} isopycnal and consider the OHC changes in a temperature framework (Walsh 1982). The change in the volume of distinct temperature classes determines the amount of water that becomes warmer

or cooler, which can then be compared to the warming or cooling predicted by air-sea heat fluxes acting over the same region (Figure 2d). The volumetric distribution in temperature classes is determined (following Marshall et al. 1993, Evans et al. 2014) by summing the total volume of grid cells that lie within each 0.5°C temperature class using an Argo-based gridded climatology (Roemmich and Gilson 2009, Boyer et al. 2013). Transformations of water across surfaces of constant temperature (isotherms) are determined by building a series of linear equations describing the volume change in each temperature class in terms of the unknown transformations and solving using a matrix inversion (Evans et al. 2014). The transformations of water across isotherms predicted by air-sea heat fluxes are determined by integrating the air-sea fluxes over the surface area of the ocean occupied by a specific temperature class (Speer 1993, Evans et al. 2014). The anomalous transformations are then integrated over the volume of water shallower than the 27.6 kg m^{-3} isopycnal, accumulated in time, then scaled by density and specific heat capacity to give units of heat content. The monthly means (using the period from 2004 to the end of 2013) are removed from the time series.

Based on this approach, Duchez et al. (2016) found that the ocean heat content reduction associated with wind-driven upwelling and ocean circulation changes were minor terms over this period. The monthly upwelling rate was computed from the wind stress curl over the same region used for the Atlantic SST anomaly, then multiplied by the temperature gradient between the surface and 700 m. While upwelling was more intense than usual, the associated heat content reduction of 0.2 GJ m^{-2} was only a small proportion of the observed 0.9 GJ m^{-2} cooling. The AMOC typically brings warm subtropical waters northward towards the subpolar regions. Using an estimate for the net northward transport across 41°N (extended from Willis 2010, based on Argo float profiles and altimetry), the AMOC was weaker 12.3 Sv over July 2013-June 2015. The reduced heat transport during the December 2013 to January 2014 period was about 0.14 PW, distributed over the subpolar gyre, and accounted for a cooling of only 0.1 GJ m^{-2} . Together, the anomalous Ekman upwelling in

the boxed region and reduced northward heat transport across the 41°N section cannot explain the observed cooling.

Discussion

The intense wintertime cooling over the subpolar gyre in the 2014/15 period, combined with a re-emergent cold anomaly set by the 2013/14 wintertime cooling explain the genesis of the 2015 cold blob, which involves physical processes on subannual timescales. Those mechanisms should not be confused with those driving the long-term warming hole on multidecadal to centennial timescales (Rahmstorf et al. 2015, Drijfhout et al. 2012). The analysis of temperature trends over the 20th century has highlighted the critical role played by a persistent AMOC weakening in cooling the subpolar North Atlantic on such timescales.

More generally, the large-scale and low frequency (multi-decadal) variability of SST and upper OHC in the North Atlantic is prominently manifested in the Atlantic Multidecadal Oscillation (AMO). Amongst other processes, the AMO is associated with changes in ocean circulation, including the AMOC and the interplay between the subtropical and subpolar gyres (McCarthy et al. 2015, Parker and Ollier 2016). As visible in Figure 1b, the AMO shifted from a positive (anomalously warm North Atlantic) to a negative phase in recent years, with the 2015 cold blob event potentially marking the starting point of an anomalously cold North Atlantic period.

The monitoring of the current North Atlantic cold blob relies on the synergy of observational systems (Argo, satellite SSTs), and its interpretation is based on the reanalysis of air-sea interactions. However, for a more complete understanding of the mechanisms driving the development of anomalous North Atlantic temperatures on both short (subannual) and long (decadal and longer) timescales, direct and sustained observations of the ocean circulation are also required. During the summer of 2014, the North Atlantic's observing system made another step with the deployment of a mooring array in the subpolar gyre ("Overturning in the Subpolar North Atlantic

Program" - OSNAP). The combination of RAPID, OSNAP, and Argo will considerably increase our knowledge of the blob's development and variability on short and long timescales, and reinforce the predictability of regional climate events, such as the 2015 Central European heat wave that followed the Atlantic cold blob.

Acknowledgments

Duchez is beneficiary of an AXA Research Fund postdoctoral grant. Desbruyères is funded by the British National Environmental Research Council (NERC - grant NE/K004387/1, DEEP-C project). Hirschi and Josey are supported by the UK NERC National Capability funding. Evan is supported by a NERC Studentship Award at the University of Southampton.

References

- Black, E. and R. Sutton, 2007: The influence of oceanic conditions on the hot European summer of 2003 *Climate Dyn.*, **28**, 53–66, doi: [10.1007/s00382-006-0179-8](https://doi.org/10.1007/s00382-006-0179-8).
- Boyer, T. P., and Coauthors, 2013: World Ocean Database 2013. NOAA Atlas NESDIS 72, Eds. S. Levitus and A. V. Mishonov, ,209pp. Available at ftp://ftp.nodc.noaa.gov/pub/WOD/DOC/wod_intro.pdf.
- Bryden, H. L., B. A. King, G. D. McCarthy, and E. L. McDonagh, 2014: Impact of a 30% reduction in Atlantic meridional overturning during 2009–2010. *Oce. Sci. Discuss.*, **11** 789–810, doi: [10.5194/os-10-683-2014](https://doi.org/10.5194/os-10-683-2014).
- Buchan, J., J.-M. Hirschi, A. T. Blaker, and B. Sinha, 2014: North Atlantic SST anomalies and the cold North European weather events of winter 2009/10 and December 2010. *Mon. Wea. Rev.*, **142**, 922–32, doi: [10.1175/MWR-D-13-00104.1](https://doi.org/10.1175/MWR-D-13-00104.1).
- Drijfhout, S., G. J. van Oldenborgh, and A. Cimatoribus, 2012: Is a decline of AMOC causing the warming hole above the North Atlantic in observed and modeled warming patterns? *J. Climate*, **25**, 8373–9, doi: [10.1175/JCLI-D-12-00490.1](https://doi.org/10.1175/JCLI-D-12-00490.1).
- Duchez, A., P. Courtois, J. J.-M. Hirschi, E. Harris, S. Josey, T. Kanzow, R. Marsh, and D. Smeed, 2015: Potential for seasonal prediction of Atlantic sea surface temperatures using the RAPID array at 26°N. *Climate Dyn.*, **46**, 3351–3370, doi: [10.1007/s00382-015-2918-1](https://doi.org/10.1007/s00382-015-2918-1).
- Duchez, A., E. Frajka-Williams, S. A. Josey, D. G. Evans, J. P. Grist, R. Marsh, G. D. McCarthy, B. Sinha, D. I. Berry, and J. J. Hirschi, 2016: Drivers of exceptionally cold North Atlantic Ocean temperatures and the 2015 European heat wave. *Environ. Res. Lett.*, submitted.
- Evans, D. G., J. D. Zika, A. C. Naveira Garabato, and A. J. G. Nurser, 2014: The imprint of Southern Ocean overturning on seasonal water mass variability in Drake Passage. *J. Geophys. Res. Ocean*, **119**, 7987–8010, doi: [10.1002/2014JC010097](https://doi.org/10.1002/2014JC010097).
- Grist, J. P., S. A. Josey, Z. L. Jacobs, R. Marsh, B. Sinha, and E. Van Sebille, 2015: Extreme air-sea interaction over the North Atlantic subpolar gyre during the winter of 2013–14 and its sub-surface legacy. *Climate Dyn.*, 1–19, doi: [10.1007/s00382-015-2819-3](https://doi.org/10.1007/s00382-015-2819-3).
- Marshall, J. C., R. G. Williams, and A. J. G. Nurser, 1993: Inferring the subduction rate and period over the North Atlantic. *J. Phys. Oceanogr.*, **23**, 1315–29, doi: [10.1175/1520-0485](https://doi.org/10.1175/1520-0485).
- McCarthy, G., I. Haigh, J. Hirschi, J. Grist, and D. Smeed, 2015: Ocean impact on decadal Atlantic climate variability revealed by sea-level observations. *Nature*, **521**, 508–510, doi: [10.1038/nature14491](https://doi.org/10.1038/nature14491).
- Nakamura, M., T. Enomoto, and S. Yamane, 2005: A simulation study of the 2003 heatwave in Europe. *J. Earth Simul.*, **2**, 55–69.
- Parker, A., and C. D. Ollier, 2016: There is no real evidence for a diminishing trend of the Atlantic meridional overturning circulation. *J. Ocean Eng. Sci.*, **1**, 30–35, doi: [10.1016/j.joes.2015.12.007](https://doi.org/10.1016/j.joes.2015.12.007).
- Rahmstorf, S., J. E. Box, G. Feulner, M. E. Mann, A. Robinson, S. Rutherford, and E. J. Schaffernicht, 2015: Exceptional twentieth-century slowdown in Atlantic Ocean overturning circulation. *Nat. Climate Change*, **5**, 475–480, doi: [10.1038/NCLIMATE2554](https://doi.org/10.1038/NCLIMATE2554).
- Roemmich, D., and J. Gilson, 2009: The 2004–2008 mean and annual cycle of temperature, salinity, and steric height in the global ocean from the Argo Program. *Prog. Oceanogr.*, **82**, 81–100, doi: [10.1016/j.pocean.2009.03.004](https://doi.org/10.1016/j.pocean.2009.03.004).
- Russo, S., J. Sillmann, and E. M. Fischer, 2015: Top ten European heatwaves since 1950 and their occurrence in the future. *Environ. Res. Lett.*, **10**, 124003, doi: [10.1088/1748-9326/10/12/124003](https://doi.org/10.1088/1748-9326/10/12/124003).
- Smeed, D. A., and Coauthors, 2014: Observed decline of the Atlantic meridional overturning circulation 2004–2012. *Ocean Sci.*, **10**, 29–38, doi: [10.5194/os-10-29-2014](https://doi.org/10.5194/os-10-29-2014).
- Speer, K. G., 1993: Conversion among North Atlantic surface water types. *Tellus A*, **45**, 72–9, doi: [10.1034/j.1600-0870.1993.00006.x](https://doi.org/10.1034/j.1600-0870.1993.00006.x).
- Sutton, R., and P.-P. Mathieu, 2002: Response of the atmosphere–ocean mixed-layer system to anomalous ocean heat-flux convergence. *Quart. J. Roy. Meteorol. Soc.*, **128**, 1259–1275, doi: [10.1256/003590002320373283](https://doi.org/10.1256/003590002320373283).
- Walin, G., 1982: On the relation between sea-surface heat flow and thermal circulation in the ocean. *Tellus*, **34**, 187–95, doi: [10.1111/j.2153-3490.1982.tb01806.x](https://doi.org/10.1111/j.2153-3490.1982.tb01806.x).

What caused the Atlantic cold blob of 2015?

Stephen G. Yeager¹, Who M. Kim¹, and Jon Robson²

¹National Center for Atmospheric Research

²University of Reading, UK

While 2015 went into the books as the warmest year ever for the planet as a whole, considerable attention has been focused on the record cold annual mean surface temperatures that were observed over the course of the same year in the high-latitude North Atlantic (e.g., Mooney 2015; Henson 2016). More often than not, coverage of the 'Atlantic cold blob' in the popular news media included a reference to the film *The Day After Tomorrow*, a farcical movie whose central plot device involves an abrupt and total shutdown of the Atlantic Ocean circulation. The narrative framing of the cold blob in terms of dramatic human-induced climate change was influenced by the publication in early 2015 of a high-profile study that argued that the Atlantic Meridional Overturning Circulation (AMOC) underwent an unprecedented slowdown during the twentieth century as a result of the melting of the Greenland Ice Sheet (Rahmstorf et al. 2015). In this article, we explore possible explanations for the record-breaking cold, review some of the recent work that has advanced our understanding of mechanisms at work in the high-latitude North Atlantic, and argue that natural climate variability offers the best explanation for the 2015 cold blob, although an anthropogenic influence cannot be discounted.

The Atlantic warming hole

Could the 2015 cold blob somehow be related to global warming associated with greenhouse gas emissions? Rahmstorf and coauthors argue that the so-called 'Atlantic warming hole' – the contrast between the observed long-

term cooling in the subpolar Atlantic and the pronounced surface warming over much of the rest of the planet – is likely caused by an unprecedented, anthropogenic slowdown of the AMOC. It seems conceivable that the record cold annual mean surface temperatures in the subpolar North Atlantic (SPNA) in 2015 (i.e., the 'cold blob') might be fundamentally related to a gradual, externally-forced relative cooling trend in the SPNA (i.e., the 'warming hole'), insofar as the latter would be conducive to record low temperatures in modern times.

We can gain some insight into the relative roles of natural and externally-forced climate variability in the SPNA by considering a 35-member ensemble of coupled climate simulations of the 20th and 21st centuries, the CESM Large Ensemble (CESM LE; Kay et al. 2015). The CESM LE ensemble mean exhibits a good correspondence with observed SPNA sea surface temperature (SST) trends over the last hundred years or so (Figure 1, panels a-c), which suggests that the long-term cooling of the SPNA is largely a response to external forcings (primarily greenhouse gases as well as natural and anthropogenic aerosols). In CESM LE, the SPNA forced response (thick black curve in Figure 1c) is dominated by a pronounced cold spell in the 1960s and recovery in the 1970s that is presumably related to both anthropogenic and naturally-occurring aerosols and a subsequent forced AMOC response (Terray 2012; Swingedouw et al. 2015). Thus, it is unclear how much of the long-term cooling trend in CESM LE is anthropogenic.

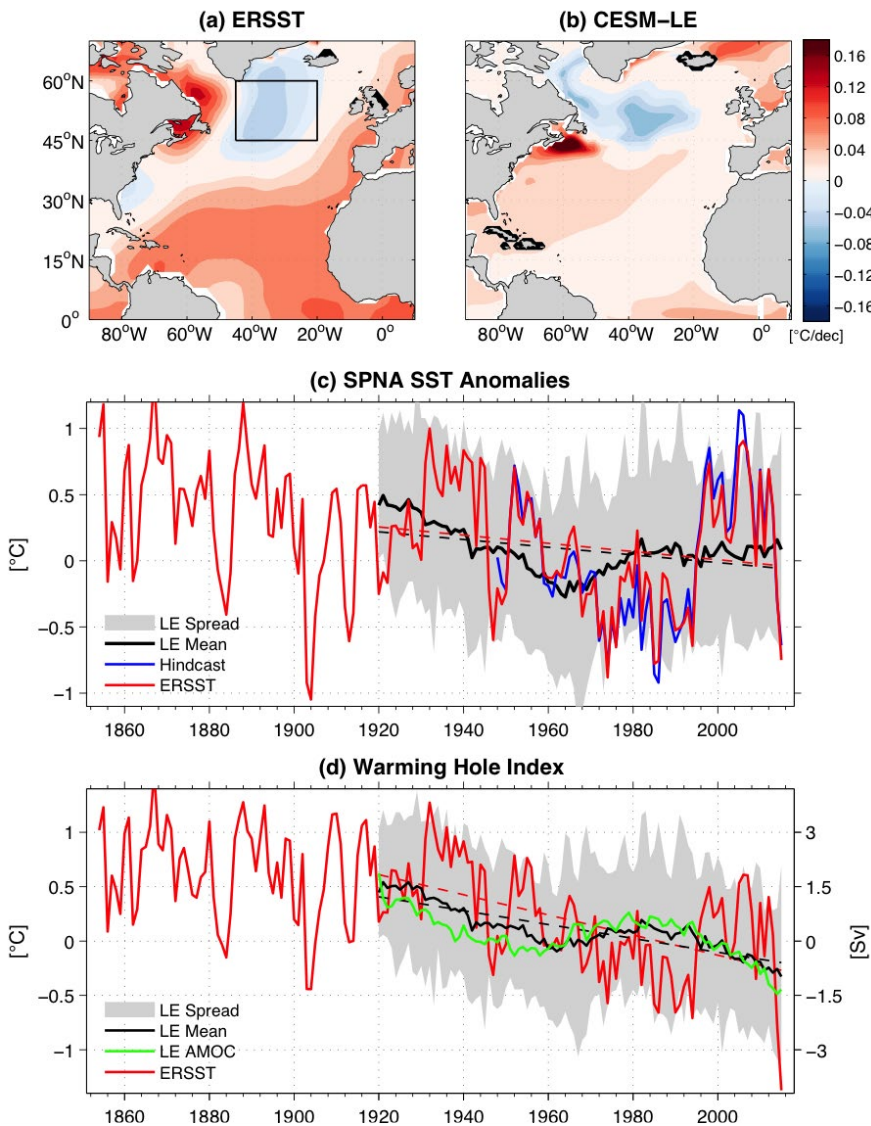


Figure 1: Linear trend of SST between 1920-2015 ($^{\circ}\text{C}/\text{decade}$) from (a) the ERSSTv4 observational dataset and (b) the average of a 35-member ensemble of 20th century coupled climate simulations (CESM LE; see text). (c) Annual SST ($^{\circ}\text{C}$) anomalies averaged over the Subpolar North Atlantic (SPNA; $45^{\circ}\text{N}-60^{\circ}\text{N}$, $45^{\circ}\text{W}-20^{\circ}\text{W}$; see box in top left panel) from (red) ERSSTv4 observations (1860-2015), (blue) a Coordinated Ocean-ice Reference Experiment (CORE) ocean-ice hindcast simulation (1948-2015; Yeager et al. 2015), and (black/grey) CESM LE ensemble mean/range (1920-2015). (d) Annual Warming Hole Index (WHI, $^{\circ}\text{C}$), computed as the difference between SPNA SST and Northern Hemisphere average SST, from ERSSTv4 and CESM LE and (green) CESM LE ensemble mean AMOC strength at 26°N (Sv). Dashed lines show long-term (1920-2015) trends of respective curves. All anomalies are relative to the respective 1948-2015 climatologies.

Assessing the role of external forcing in creating favorable conditions for the 2015 cold blob is quite nuanced because the modest downward trend in SPNA SST is likely the net result of compensating tendencies: a direct radiatively-forced warming and an indirect AMOC-driven cooling (Drijfhout et al. 2012). A warming hole index (WHI), similar to that shown in Rahmstorf et al. (2015), which quantifies the evolution of SPNA SST relative to the Northern Hemisphere average SST, serves to highlight these competing tendencies (Figure 1d). The observed WHI trend is considerably more negative than the SPNA SST trend, reflecting the fact that the SPNA has cooled while the Northern Hemisphere surface ocean has warmed, on average, over the historical record. The CESM LE suggests that an externally-forced weakening of the AMOC (-1.3 Sv/century) has contributed to a deepening of the warming hole in the last century (compare green/black curves in Figure 1d; their correlation is 0.8), in line with other studies (Drijfhout et al. 2012; Rahmstorf et al. 2015). The externally-forced WHI trend over the period 1920-2015 diagnosed from CESM LE ($-0.64^{\circ}\text{C}/\text{century}$; black dashed line in Figure 1d) is less than the observed trend ($-0.93^{\circ}\text{C}/\text{century}$; red dashed line in same Figure), but the latter does fall within the distribution of WHI trends computed from individual CESM LE ensemble members (not shown). The CESM LE distribution of WHI trends implies that part of the observed WHI trend is associated with internal climate variability, but, to a large extent, the absence of warming in the SPNA over the 20th Century can be interpreted as a reflection of the forced response of the

climate system. Therefore, the CESM LE simulations lend some support to the hypothesis that an externally-forced slowdown in AMOC (which future scenario simulations would strongly suggest is anthropogenic) has probably played a role in the 2015 cold blob by deepening the warming hole and preconditioning the SPNA for record lows to occur through intrinsic climate processes.

While the warming hole phenomenon is certainly germane to the question of “what caused the Atlantic cold blob?”, it doesn’t contribute much to our understanding of how and why record cold anomalies were observed last year in particular. Regardless of the drivers of the forced variability (anthropogenic or natural), the large spread across ensemble members (grey shading in Figure 1c) clearly demonstrates the dominance of internal climate variability in the SPNA region in coupled climate simulations of the 20th century, which is a well-known result (Terray 2012). Thus, while the observed long-term cooling trend (or absence of warming) may well be related to greenhouse gas forcing, the fraction of observed SPNA SST variance explained is very small, especially on decadal timescales (Figure 1c, compare red curve with corresponding trend line).

Attributing the 2015 cold blob to specific processes and mechanisms is complicated by the fact that the SPNA is a highly variable region influenced by multiple drivers operating on a wide range of timescales. The SPNA is dominated by large amplitude decadal SST fluctuations (Figure 1c). In coupled climate model simulations, such low-frequency variability is intrinsic (grey shading in Figure 1c) and can be causally linked to changes in the strength of AMOC-related ocean heat transport (e.g., Delworth and Mann 2000; Knight et al. 2005) driven by high-latitude air-sea fluxes (Delworth and Zeng 2016). In our opinion, the most compelling explanation for the 2015 cold blob is to be found in the recent history of atmospheric variability over the North Atlantic and its imprint on the large-scale Atlantic Ocean circulation.

The role of the North Atlantic Oscillation

We lack the observations that would be needed to

establish a definitive link between ocean dynamics and observed SPNA surface temperatures on multidecadal timescales. However, a host of modeling studies (e.g., Häkkinen 1999; Delworth and Greatbatch 2000; Eden and Willebrand 2001; Bentsen et al. 2004; Beismann and Barnier 2004; Boning et al. 2006; Blaustoch et al. 2008, Lohmann et al. 2009a; Robson et al. 2012a; Yeager and Danabasoglu 2014; Danabasoglu et al. 2016) consistently suggest that large, multidecadal changes in the strength of AMOC, subpolar gyre circulation, and related ocean heat transport into the SPNA in the 20th century were associated with the historical variability of the North Atlantic Oscillation (NAO) – the dominant mode of atmospheric variability in the North Atlantic. A recent study of sea-level gauge data (McCarthy et al. 2015) lends observational support to the model-based evidence that slow variations in the Atlantic thermohaline circulation (THC) associated with time-integrated NAO forcing played an important role in driving the large decadal swings in observed SPNA temperature seen in Figure 1.

Strong winter positive NAO conditions are associated with intense cooling of the SPNA via enhanced turbulent heat loss and anomalous Ekman transport (Marshall et al. 2001; Deser et al. 2010). While the immediate effect of this forcing is to reduce SST in the SPNA, persistent positive NAO conditions over several consecutive winters will tend to enhance the production of Labrador Sea Water (Yashayaev 2007), strengthening the THC and augmenting the ocean heat convergence into the SPNA (Lohmann et al. 2009a,b; Delworth and Zeng 2016). The SPNA cooling (warming) trend in the 1960s (1990s) has been linked to anomalously weak (strong) AMOC/THC conditions (Grist et al. 2010; Robson et al. 2012a; Yeager et al. 2012; Robson et al. 2014a) that largely reflect the cumulative NAO-forcing history of prior years (Figure 2a). A heat budget of the SPNA upper ocean from an ocean-ice hindcast simulation forced with atmospheric reanalysis fields (see Danabasoglu et al. 2016 for a detailed description), whose SPNA SST representation exhibits excellent agreement with the observed SST (Figure 1c), demonstrates the dominate role of large, decadal changes in ocean heat convergence (blue curve in Figure

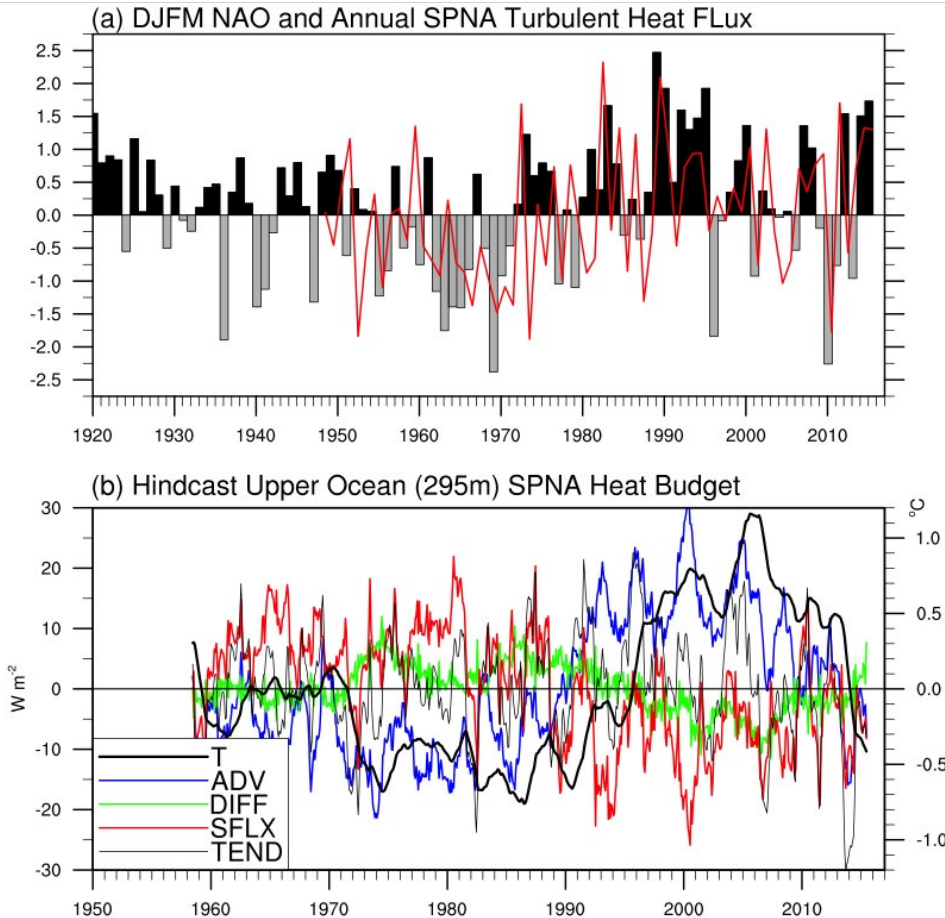


Figure 2: (a) Station-based observed winter (DJFM) NAO index through 2015 (black/grey bars; <https://climatedataguide.ucar.edu/climate-data/hurrell-north-atlantic-oscillation-nao-index-station-based>), and an observation-based estimate of the annual mean turbulent surface heat flux (red; positive values tend to cool the ocean) averaged over the SPNA box (see Figure 1). Both time series have been normalized by their respective standard deviations. The turbulent heat flux is computed as in Large and Yeager (2009) but using ERSSTv4 for SST. The correlation of the two time series is 0.39, which is significant at the 99% level. (b) Monthly heat budget for the SPNA region (to a depth of 295 m) from the CORE ocean-ice hindcast simulation. The ocean heat budget tendencies (referring to left axis, positive values tend to warm the ocean, Wm^{-2}) are as follows: (grey) total, (blue) advection, (green) diffusion, and (red) net surface heat flux. The volume-average temperature of the box (T , thick black) is the time-integral of the tendency and refers to the right axis ($^{\circ}\text{C}$). All budget terms have been smoothed with a 12-month running mean. Anomalies are relative to a 1948-2015 climatology in (a) and relative to a 1958-2015 climatology in (b).

2b) that are largely associated with NAO forcing.

A number of recent decadal prediction studies have shown that the large SPNA temperature shifts of the 1960s and 1990s can be retrospectively predicted using coupled climate simulations initialized from historical ocean states (e.g., Robson et al. 2012b; Yeager et al. 2012; Msadek et al. 2014; Robson et al. 2014a; Hermanson et al. 2014; Yeager et al. 2015). Although the NAO itself is not skillfully predicted in such forecast systems, the prior history of NAO forcing is inherent in the ocean initial conditions. Slow-evolving, historical THC anomalies are embedded in the coupled model solution through initialization, and the associated ocean heat transport anomalies drive realistic SPNA upper ocean temperature changes at multi-year forecast lead times (Figure 3, panels b and d). The fact that decadal SPNA temperature variability can be predicted in advance lends strong support to the argument that ocean dynamics play a dominant role in driving the observed SPNA temperature changes (O'Reilly et al. 2016).

Although decadal climate prediction is still a new and rapidly evolving science, a number of studies published within the last two years (prior to or concurrent with the cold blob) anticipated a transition to a colder decadal regime in the SPNA than has prevailed since the turn of

the century (Figure 1c). Robson et al. (2014b) argued that the observed downward trend in AMOC measured at 26.5°N (Smeed et al. 2014) may be a reflection of a substantial and ongoing decline in AMOC strength associated with a recent sharp decrease in observed Labrador Sea density from the highs of the late 1990s. The frequent neutral or negative winter NAO conditions after 1996 (Figure 2a) contributed to a relative deficit of deep water formation in recent years, and the weakened THC results in SPNA cooling trends in the most recent decadal forecasts made using initialized coupled climate models (Hermanson et al. 2014; Yeager et al. 2015; see also Figure 3). These model-based forecasts are consistent with predictions based on recent observed sea level changes along the east coast of North America (McCarthy et al. 2015).

A confluence of slow and fast timescale responses to NAO forcing

The recent THC weakening and associated ocean-driven cooling of the SPNA is linked to the cumulative effect of frequent weak and negative NAO winters between 1996 and 2013 (Yeager et al. 2015). However, the strong positive NAO conditions in recent years (Figure 2; the December through March NAO index exceeded +1 std. dev. in the winters of 2014 and 2015) likely contributed to greatly enhanced cooling rates in the SPNA through anomalous air-sea heat flux and Ekman effects (Marshall et al. 2001). In particular, the NAO index in 2015 was the highest since 1995. The observation-based estimate of surface turbulent heat flux shown in Figure 2a suggests that 2014–2015 was the two-year stretch with the most intense surface heat loss from the SPNA upper ocean since the late 1980s. The hindcast heat budget (Figure 2b) suggests that an unprecedented cooling

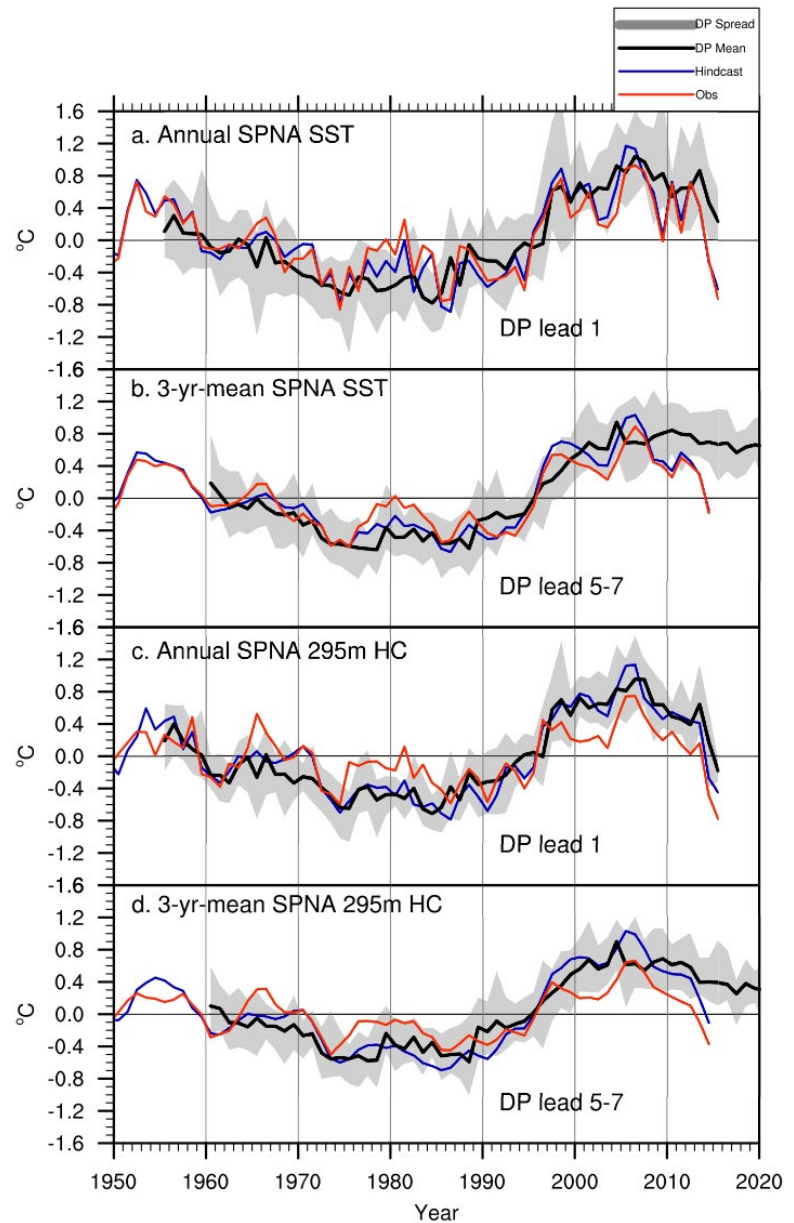


Figure 3: Time series of SPNA (see Figure 1 box) anomalies of (a, b) SST ($^{\circ}$ C) from: (red) observations, (blue) CORE ocean-ice hindcast simulation, and (black/grey) 10-member CESM initialized decadal prediction (DP) simulations (see Yeager et al. 2015). Panels (a,c) show predicted anomalies for forecast lead year 1 (e.g., the final point on the black curve shows the predicted 2015 anomaly based on simulations initialized on Nov. 1, 2014). Panels (b,d) show predicted 3-year anomalies for forecast lead years 5–7 (e.g., the predicted 2013–2015 anomaly is based on simulations initialized on Nov. 1, 2008; the final point on the black curves shows the predicted 2019–2021 anomaly based on simulations initialized on Nov. 1, 2014). In panels a and b, ERSSSTv4 observations are used, while in panels c and d, the red curve is based on the UK Met Office EN4.1.1 objectively analyzed temperature data (Good et al. 2013). All anomalies are relative to the respective 1964–2014 climatologies, and this climatology is a function of forecast lead time for the decadal predictions.

occurred in the winter of 2014 that was due to both intense air-sea heat loss and a precipitous drop in ocean advective heat convergence (in particular, a sharp drop in heat transport from the south, not shown, that we think may be related to anomalous Ekman transport). The winter of 2015 then resulted in a further, less dramatic cooling that was sufficient to push surface temperatures into record territory. We propose that the best explanation at this time for the Atlantic cold blob of 2015 was that it was the result of constructive responses to intrinsic NAO variability operating at distinct timescales: 1) a slow and persistent ocean-driven reduction of SPNA upper ocean heat content reflecting THC spindown and weak NAO forcing in the post-1995 decades, and 2) a fast atmospheric extraction of heat and perturbation of surface ocean currents (Ekman transport) associated with the recent strong winter positive NAO conditions.

Future work will undoubtedly shed much more light on this dramatic cooling of the North Atlantic, which saw a two-year decrease in SPNA surface temperatures that was as large as the increase observed during the mid-1990s. While the CESM decadal prediction system is generally skillful at predicting the slow evolution of SPNA SST, a 10-member ensemble that was initialized on November 1, 2014, was not able to anticipate the magnitude of the surface cooling that actually occurred in 2015 (Figure 3a). The ocean hindcast simulation which provided the ocean and sea ice initial conditions for the predictions may have overestimated the magnitude of recent positive upper ocean heat content anomalies (Figure 3c; note that objectively analyzed temperature reconstructions also have uncertainty). Recent short-term predictions of 295 m SPNA heat content exhibit a closer match to the historical reconstructions, due to persistence, but still fail to encompass either the hindcast-simulated or observation-based anomaly for 2015. This raises a number of questions that will need to be pursued. Would better initialization improve the predictions of this event? Could it be that rapid SPNA warmings are more predictable than rapid coolings? Are there inherent deficiencies in the simulation and prediction of NAO in this class of coupled model? Is a 10-member

decadal prediction ensemble too small to encompass such events? Were the strong positive NAO conditions of 2014 and 2015, and associated rapid SPNA SST changes, random natural variations or might they reflect a forced response (e.g., Gastineau and Frankignoul 2015; Gray et al. 2013)?

Finally, we note that the last few consecutive years of strong positive NAO forcing (including the most recent winter of 2016) can be expected to replenish the supply of North Atlantic deep water that comprises the lower limb of the AMOC. Recent observations in the Labrador Sea indicate that there has been a dramatic resumption of deep convection there (Yashayaev and Loder 2016), presumably related to recent atmospheric conditions. If strong deep water formation continues in coming years, a reinvigorated THC would eventually act to warm the subpolar North Atlantic, in stark contrast to the Hollywood ending.

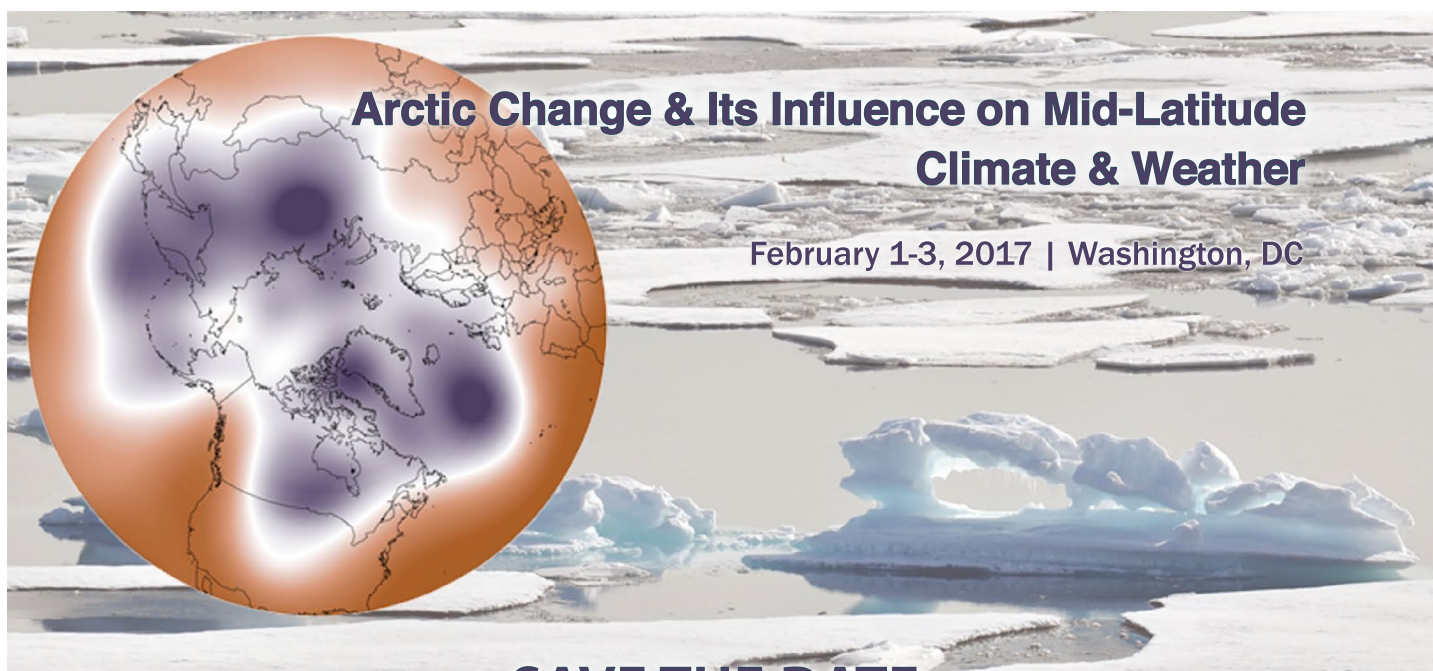
Acknowledgments

This work was supported by the National Oceanic and Atmospheric Administration (NOAA) Climate Program Office under Climate Variability and Predictability Program grants NA09OAR4310163 and NA13OAR4310138, by the National Science Foundation (NSF) Collaborative Research EaSM2 grant OCE-1243015, and by the NSF through its sponsorship of the National Center for Atmospheric Research. We thank Clara Deser and Jennifer Kay for leading the CESM Large Ensemble project, and to Nan Rosenbloom and Keith Lindsay for running the CORE ocean-ice hindcast and CESM decadal prediction experiments. These simulations used computing resources of the National Energy Research Scientific Computing Center (NERSC) which is supported by the US Department of Energy, as well as resources provided by NCAR's Computational and Information Systems Laboratory (CISL).

References

- Beissmann, J.-O., and B. Barnier, 2004: Variability of the meridional overturning circulation of the North Atlantic: Sensitivity to overflows of dense water masses. *Ocean Dyn.*, **54**, 92-106, doi:[10.1007/s10236-003-0088-x](https://doi.org/10.1007/s10236-003-0088-x).
- Biastoch, A., C. Böning, J. Getzlaff, J.-M. Molines, and G. Madec, 2008: Causes of interannual-decadal variability in the meridional overturning circulation of the midlatitude North Atlantic Ocean. *J. Climate*, **21**, 6599-6615, doi: [10.1175/2008JCLI2404.1](https://doi.org/10.1175/2008JCLI2404.1).
- Böning, C., M. Scheinert, J. Dengg, A. Biastoch, and A. Funk, 2006: Decadal variability of subpolar gyre transport and its reverberation in the North Atlantic overturning. *Geophys. Res. Lett.*, **33**, L21S01, doi: [10.1029/2006GL026906](https://doi.org/10.1029/2006GL026906).
- Bentsen, M., H. Drange, T. Furevik, and T. Zhou, 2004: Simulated variability of the Atlantic meridional overturning circulation. *Climate Dyn.*, **22**, 701-720, doi: [10.1007/s00382-004-0397-x](https://doi.org/10.1007/s00382-004-0397-x).
- Danabasoglu, G., and Coauthors, 2016: North Atlantic simulations in Coordinated Ocean-Ice Reference Experiments phase II (CORE-II). Part II: Inter-annual to decadal variability. *Ocean Model.*, **97**, 65-90, doi: [10.1016/j.ocemod.2015.11.007](https://doi.org/10.1016/j.ocemod.2015.11.007).
- Delworth, T. L., and R. J. Greatbatch, 2000: Multidecadal thermohaline circulation variability driven by atmospheric surface flux forcing. *J. Climate*, **13**, 1481-1495, doi: [10.1175/1520-0442\(2000\)013<1481:2.0.CO;2](https://doi.org/10.1175/1520-0442(2000)013<1481:2.0.CO;2).
- Delworth, T. L., and M. E. Mann, 2000: Observed and simulated multidecadal variability in the Northern Hemisphere. *Climate Dyn.*, **16**, 661-676, doi: [10.1007/s003820000075](https://doi.org/10.1007/s003820000075).
- Delworth, T. L., and F. Zeng, 2016: The impact of North Atlantic Oscillation on climate through its influence on the Atlantic Meridional Overturning Circulation. *J. Climate*, **29**, 941-962, doi: [10.1175/JCLI-D-15-0396.1](https://doi.org/10.1175/JCLI-D-15-0396.1).
- Deser, C., M. A. Alexander, S.-P. Xie, and A. S. Phillips, 2010: Sea surface temperature variability: Patterns and mechanisms. *Ann. Rev. Marine Sci.*, **2**, 115-143, doi: [10.1146/annurev-marine-120408-151453](https://doi.org/10.1146/annurev-marine-120408-151453).
- Drijfhout, S., G. J. van Oldenborgh, and A. Cimatoribus, 2012: Is a decline of AMOC causing the warming hole above the North Atlantic in observed and modeled warming patterns? *J. Climate*, **25**, 8373-8379, doi: [10.1175/JCLI-D-12-00490.1](https://doi.org/10.1175/JCLI-D-12-00490.1).
- Eden, C., and J. Willebrand, 2001: Mechanism of interannual to decadal variability of the North Atlantic circulation. *J. Climate*, **14**, 2266-2280, doi: [10.1175/1520-0442\(2001\)014<2266:MOITDV>2.0.CO;2](https://doi.org/10.1175/1520-0442(2001)014<2266:MOITDV>2.0.CO;2).
- Gastineau, G., and C. Frankignoul, 2015: Influence of the North Atlantic SST variability on the atmospheric circulation during the twentieth century. *J. Climate*, **28**, 1396-1416, doi: [10.1175/JCLI-D-14-00424.1](https://doi.org/10.1175/JCLI-D-14-00424.1).
- Good, S. A., M. J. Martin, and N. A. Rayner, 2013: EN4: quality controlled ocean temperature and salinity profiles and monthly objective analyses with uncertainty estimates. *J. Geophys. Res. Oceans*, **118**, 6704-6716, doi: [10.1002/2013JC009067](https://doi.org/10.1002/2013JC009067).
- Gray, L. J., A. A. Scaife, D. M. Mitchell, S. Osprey, S. Ineson, S. Hardiman, N. Butchart, J. Knight, R. Sutton, and K. Kodera, 2013: A lagged response to the 11 year solar cycle in observed winter Atlantic/European weather patterns. *J. Geophys. Res. Atmos.*, **118**, 13405-13420, doi: [10.1002/2013JD020062](https://doi.org/10.1002/2013JD020062).
- Grist, J. P., S. A. Josey, R. Marsh, S. A. Good, A. C. Coward, B. A. de Cuevas, S. G. Alderson, A. L. New, and G. Madec, 2010: The roles of surface heat flux and ocean heat transport convergence in determining Atlantic Ocean temperature variability. *Ocean Dyn.*, **60**, 771-790, doi: [10.1007/s10236-010-0292-4](https://doi.org/10.1007/s10236-010-0292-4).
- Häkkinen, S., 1999: Variability of the simulated meridional heat transport in the North Atlantic for the period 1951-1993. *J. Geophys. Res.*, **104**, 10991-11007, doi: [10.1029/1999JC900034](https://doi.org/10.1029/1999JC900034).
- Henson, B., 2016: The North Atlantic Blob: A marine cold wave that won't go away. *Weather Underground*, Accessed 8 April 2016. [Available at: www.wunderground.com/blog/JeffMasters/the-north-atlantic-blob-a-marine-cold-wave-that-wont-go-away/.]
- Hermanson, L., R. Eade, N. H. Robinson, N. J. Dunstone, M. B. Andrews, J. R. Knight, A. A. Scaife, and D. M. Smith, 2014: Forecast cooling of the Atlantic subpolar gyre and associated impacts. *Geophys. Res. Lett.*, **41**, 5167-5174, doi: [10.1002/2014GL060420](https://doi.org/10.1002/2014GL060420).
- Kay, J., and Coauthors, 2015: The Community Earth System Model (CESM) Large Ensemble Project: A community resource for studying climate change in the presence of internal climate variability. *Bull. Amer. Meteorol. Soc.*, **96**, 1333-1349, doi: [10.1175/BAMS-D-13-00255.1](https://doi.org/10.1175/BAMS-D-13-00255.1).
- Knight, J. R., R. J. Allan, C. K. Folland, M. Vellinga, and M. E. Mann, 2005: A signature of persistent natural thermohaline circulation cycles in observed climate. *Geophys. Res. Lett.*, **32**, L20708, doi: [10.1029/2005GL024233](https://doi.org/10.1029/2005GL024233).
- Large, W. G., and S. G. Yeager, 2009: The global climatology of an interannually varying air-sea flux data set. *Climate Dyn.*, **33**, 341-364, doi: [10.1007/s00382-008-0441-3](https://doi.org/10.1007/s00382-008-0441-3).
- Lohmann, K., H. Drange, and M. Bentsen, 2009a: Response of the North Atlantic subpolar gyre to persistent North Atlantic Oscillation forcing. *Climate Dyn.*, **32**, 273-285, doi: [10.1007/s00382-008-0467-6](https://doi.org/10.1007/s00382-008-0467-6).
- Lohmann, K., H. Drange, and M. Bentsen, 2009b: A possible mechanism for the strong weakening of the North Atlantic subpolar gyre in the mid-1990s. *Geophys. Res. Lett.*, **36**, L15602, doi: [10.1029/2009GL039166](https://doi.org/10.1029/2009GL039166).
- Marshall, J., H. Johnson, and J. Goodman, 2001: A study of the interaction of the North Atlantic Oscillation with ocean circulation. *J. Climate*, **14**, 1399-1421, doi: [10.1175/1520-0442\(2001\)014<1399:ASOTIO>2.0.CO;2](https://doi.org/10.1175/1520-0442(2001)014<1399:ASOTIO>2.0.CO;2).
- McCarthy, G. D., I. D. Haigh, J. J.-M. Hirschi, J. P. Grist, and D. A. Smeed, 2015: Ocean impact on decadal Atlantic climate variability revealed by sea-level observations. *Nature*, **521**, 508-510, doi: [10.1038/nature14491](https://doi.org/10.1038/nature14491).
- Mooney, C., 2015: Everything you need to know about the surprisingly cold 'blob' in the North Atlantic ocean. *The Washington Post*, Accessed on 30 September 2015. [Available at: www.washingtonpost.com/news/energy-environment/wp/2015/09/30/everything-you-need-to-know-about-the-cold-blob-in-the-north-atlantic-ocean/.]
- Msadek, R., and Coauthors, 2014: Predicting a decadal shift in North Atlantic climate variability using the GFDL forecast system. *J. Climate*, **27**, doi: [10.1175/JCLI-D-13-00476.1](https://doi.org/10.1175/JCLI-D-13-00476.1).
- O'Reilly, C. H., M. Huber, T. Woollings, and L. Zanna, 2016: The signature of low-frequency oceanic forcing in the Atlantic Multidecadal Oscillation. *Geophys. Res. Lett.*, **43**, doi: [10.1002/2016GL067925](https://doi.org/10.1002/2016GL067925).
- Rahmstorf, S., J. E. Box, G. Feulner, M. E. Mann, A. Robinson, S. Rutherford, and E. J. Schaffernicht, 2015: Exceptional twentieth-century slowdown in Atlantic Ocean overturning circulation. *Nat. Climate Change*, **5**, 475-480, doi: [10.1038/NCLIMATE2554](https://doi.org/10.1038/NCLIMATE2554).

- Robson, J. I., R. Sutton, K. Lohmann, D. Smith, and M. D. Palmer, 2012a: Causes of the rapid warming of the North Atlantic Ocean in the mid-1990s. *J. Climate*, **25**, 4116-4134, doi:[10.1175/JCLI-D-11-00443.1](https://doi.org/10.1175/JCLI-D-11-00443.1).
- Robson, J. I., R. Sutton, and D. Smith, 2012b: Initialized decadal predictions of the rapid warming of the North Atlantic Ocean in the mid 1990s. *Geophys. Res. Lett.*, **39**, doi:[10.1029/2012GL053370](https://doi.org/10.1029/2012GL053370).
- Robson, J., R. Sutton, and D. Smith, 2014a: Decadal predictions of the cooling and freshening of the North Atlantic in the 1960s and role of ocean circulation. *Climate Dyn.*, **42**, 2353-2365, doi:[10.1007/s00382-014-2115-7](https://doi.org/10.1007/s00382-014-2115-7).
- Robson, J., D. Hodson, E. Hawkins, and R. Sutton, 2014b: Atlantic overturning in decline? *Nat. Geosci.*, **7**, 2-3, doi:[10.1038/ngeo2050](https://doi.org/10.1038/ngeo2050).
- Smeed, D. A., and Coauthors, 2014: Observed decline of the Atlantic meridional overturning circulation 2004-2012. *Ocean Sci.*, **10**, 29-38, doi:[10.5194/os-10-29-2014](https://doi.org/10.5194/os-10-29-2014).
- Swingedouw, D., P. Ortega, J. Mignot, E. Guilyardi, V. Masson-Delmotte, P. G. Butler, M. Khodri, and R. Séférian, 2015: Bidecadal North Atlantic ocean circulation variability controlled by timing of volcanic eruptions. *Nat. Comm.*, **6**:6545, doi:[10.1038/ncomms7545](https://doi.org/10.1038/ncomms7545).
- Terray, L., 2012: Evidence for multiple drivers of North Atlantic multi-decadal climate variability. *Geophys. Res. Lett.*, **39**, L19712, doi:[10.1029/2012GL053046](https://doi.org/10.1029/2012GL053046).
- Yashayaev, I., 2007: Hydrographic changes in the Labrador Sea, 1960-2005. *Prog. Oceanogr.*, **73**, 242-276, doi:[10.1016/j.pocean.2007.04.015](https://doi.org/10.1016/j.pocean.2007.04.015).
- Yashayaev, I., and J. W. Loder, 2016: Recurrent deep convection and variable intermediate-layer water properties in the Labrador Sea. *Geophys. Res. Lett.*, submitted.
- Yeager, S., A. Karspeck, G. Danabasoglu, J. Tribbia, and H. Teng, 2012: A decadal prediction case study: Late twentieth-century North Atlantic Ocean heat content. *J. Climate*, **25**, 5173-5189, doi:[10.1175/JCLI-D-11-00595.1](https://doi.org/10.1175/JCLI-D-11-00595.1).
- Yeager, S., and G. Danabasoglu, 2014: The origins of late-twentieth-century variations in the large-scale North Atlantic circulation. *J. Climate*, **27**, 3222-3247, doi: [10.1175/JCLI-D-13-00125.1](https://doi.org/10.1175/JCLI-D-13-00125.1).
- Yeager, S. G., A. Karspeck, and G. Danabasoglu, 2015: Predicted slowdown in the rate of Atlantic sea ice loss. *Geophys. Res. Lett.*, **42**, doi:[10.1002/2015GL065364](https://doi.org/10.1002/2015GL065364).



Arctic Change & Its Influence on Mid-Latitude Climate & Weather

February 1-3, 2017 | Washington, DC

SAVE THE DATE

The Arctic has warmed more than twice as fast as the global average, experienced rapid loss of sea ice, and collapse of warm season snow cover. These profound changes to the Arctic system have coincided with a period of ostensibly more frequent events of extreme weather across the mid-latitudes, including extreme heat and rainfall events and recent severe winters.

Join us in this workshop to explore the possible links between Arctic change and mid-latitude climate and weather that has spurred a rush of new observational and modeling studies.

Greenland Ice Sheet melting influence on the North Atlantic

Andreas Schmittner¹, Pepijn Bakker^{1,2}, Rebecca Lynn Beadling³, Jan T. M. Lenaerts⁴, Sebastian Mernild^{5,6}, Oleg Saenko⁷, and Didier Swingedouw⁸

¹Oregon State University

²University of Bremen, Germany

³University of Arizona

⁴Utrecht University, Netherlands

⁵Sogn og Fjordane University College, Norway

⁶Universidad de Magallanes, Chile

⁷Canadian Centre for Climate Modeling and Analysis

⁸University of Bordeaux, France

Ever since the pioneering numerical experiments by Manabe and Stouffer (1993; 1994) it has been known that the Atlantic Meridional Overturning Circulation (AMOC; which is associated with northward flow near the surface, sinking in the North Atlantic, and return flow at depths) could be sensitive to anthropogenic carbon dioxide (CO_2) emissions. In their idealized $2\times\text{CO}_2$ climate model simulation of multi-centennial duration the AMOC reduced but eventually it recovered, whereas it disappeared altogether in their $4\times\text{CO}_2$ experiment. Manabe and Stouffer attributed the AMOC reduction to increased poleward water vapor transport in a warmer atmosphere, which increases the freshwater input to the high-latitude surface ocean, making surface waters less salty and more buoyant, and therefore less likely to sink. Although they neglected freshwater fluxes from melting land-ice in their simulations, they estimated that surface melting of the Greenland Ice Sheet (GIS) would contribute $\sim 0.1 \text{ Sv}$ ($1 \text{ Sv} = 106 \text{ m}^3\text{s}^{-1}$) in their $4\times\text{CO}_2$ experiment, whereas freshwater fluxes from the atmosphere were more than twice that. Thus Manabe and Stouffer concluded that the AMOC reduction produced by their model was a conservative estimate; in

the real world larger changes could be expected due to ice sheet melting. But they also concluded that increased poleward moisture transport was more important than GIS melting. They also examined the surface temperature response in their model and found that, even though high-latitudes in general warmed more than average, there was a distinct minimum warming in the North Atlantic and Southern Ocean, which they attributed to mixing with the deep ocean. The minimum warming in the North Atlantic has since been referred to as the warming hole, which is related to the shorter-term phenomenon of the cold blob ([see Ducharé et al., this issue](#)) as discussed by [Yeager et al. \(this issue\)](#). Although controversial, AMOC changes have been suggested as a possible cause for both, the warming hole and the cold blob. Here we focus on long term effects of GIS melt on AMOC evolution and the warming hole.

Subsequent research has largely confirmed Manabe and Stouffer's results. More recent model simulations, such as those performed for the assessment reports of the Intergovernmental Panel on Climate Change (IPCC), show a similar sensitivity to warming, where moderate

warming leads to a moderate AMOC reduction with eventual stabilization or recovery, whereas large warming can lead to very substantial AMOC declines and, in some cases, irreversible demises (Cheng et al. 2013; Schmittner et al. 2005; Weaver et al. 2012). Some progress has been made in attributing the simulated AMOC changes. Gregory et al. (2005) showed that, although freshwater fluxes contribute, the AMOC reduction in the models they examined, as well as the spread between models, was dominated by changes in surface heat fluxes, in contrast to Manabe and Stouffer who emphasized the role of freshwater fluxes. However, the most recent IPCC-type climate models used in these studies still do not include interactive ice sheets and therefore neglect the impact of ice sheet melting and the associated freshwater fluxes.

Influence of GIS melting on the AMOC

Progress has also been made recently in better estimating the surface melt contribution from the GIS. Recent measurements of the GIS mass balance indicate accelerated melting in the last few decades (Rignot et al. 2011). If this acceleration would continue, it could lead to freshwater release on the order of ~0.065 Sv by 2100 (Swingedouw et al. 2013). Based on simulations with a regional climate model at high spatial resolution (~11 km), coupled with a snow model, Lenaerts et al. (2015) estimate ~1,500 Gt/yr or ~0.05 Sv of additional freshwater flux after year 2100 for the business-as-usual RCP8.5 high carbon emission scenario, about half of Manabe and Stouffer's estimate (Figure 1). Hosing experiments with freshwater flux perturbations only (without warming) indicate that fluxes of that order of magnitude could affect the AMOC, although larger fluxes ~0.1-0.3 Sv are typically required for a substantial

reduction or a complete collapse (e.g., Rahmstorf et al. 2005). Several single model studies exploring GIS melt, in addition to global warming, and multi-model studies with idealized forcings yield different results, from negligible effects to major impacts. Collectively these studies indicate that the AMOC response depends strongly on the applied additional GIS meltwater forcing. For freshwater fluxes < 0.1 Sv and/or relatively short durations (decades) of the forcing, the AMOC response is typically small (~1-2 Sv; Lenaerts et al. 2015; Mikolajewicz et al. 2007; Swingedouw et al. 2015), whereas for larger and/or longer forcings, a substantial additional decline is simulated (Hu et al. 2009; Hu et al. 2011; Swingedouw and Braconnot 2007; Swingedouw et al. 2006). The recent study by Hansen et al. (2016) is exceptional in using a much larger freshwater forcing (> 1 Sv) than others, which causes their model's AMOC to collapse within the 21st century. However, their freshwater forcing, which is exponential and limited in duration by a five meter sea level rise, is hypothetical and not based on physical process modeling. It will be difficult to reconcile such large melt-rates with the much smaller fluxes from the

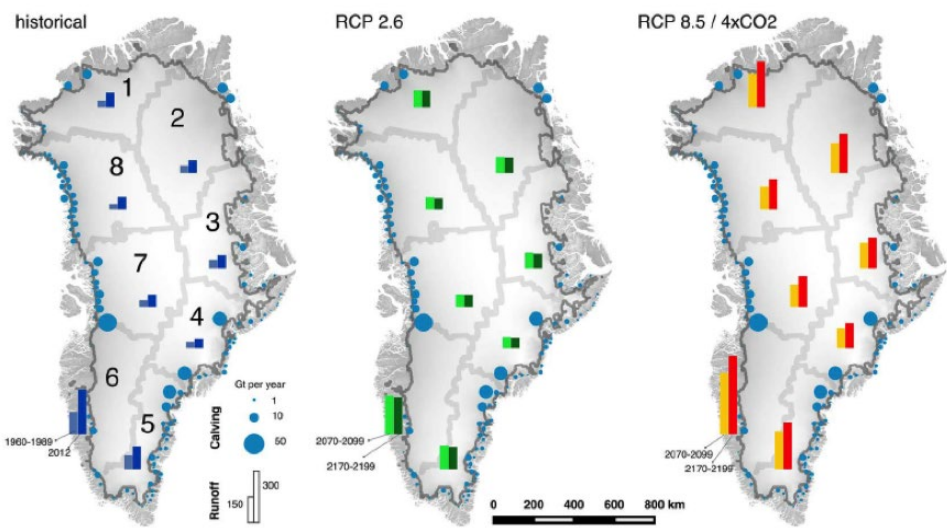


Figure 1: Runoff into eight drainage basins (bars) and glacier discharge (circles) from the GIS (in Gt/year). Left: historical estimates. Center and right: future projections, RCP2.8 and RCP8.5 respectively. From Lenaerts et al. (2015).

detailed estimates of surface mass balance mentioned above.

Realistic projections of effects of GIS melting on the AMOC are currently investigated within the [AMOC Model Intercomparison Project](#) (AMOCMIP), which uses detailed estimates of surface meltwater fluxes realistically distributed around the GIS margin according to the corresponding drainage basins (Figure 1) following the method used by Lenaerts et al. (2015) and using the CMIP5 mean atmospheric warming evolution. The resulting freshwater fluxes from Greenland, which increase from ~ 0 Sv in year 2000 to ~ 0.015 Sv (RCP4.5) and ~ 0.07 Sv (RCP8.5) in year 2300, are then fed into state-of-the-science climate models to assess their impacts on AMOC and climate. Seven of those models have already performed simulations, many until the year 2300, and submitted data. The results regarding AMOC projections will be published soon elsewhere (Bakker et al. in prep).

Influence of GIS melting on North Atlantic sea surface salinities and temperatures

Here we use AMOCMIP results to explore effects of GIS melting on surface properties in the North Atlantic. Two carbon emission scenarios were considered in AMOCMIP: the intermediate RCP4.5 and the business-as-usual RCP8.5. Simulations were performed with (labeled e.g., RCP8.5GIS in the following) and without (labeled e.g., RCP8.5) GIS melting. Differences between the two simulations quantify the effect of GIS melting. For simplicity we show results from one model only, the relatively coarse resolution (T42) OSU Vic model (Schmittner et al. 2011). GIS melting does not affect the AMOC appreciably in these

simulations. It is within ± 1 Sv of the simulations without GIS melting. Therefore the impacts of GIS melt on surface properties discussed in the following are not caused at the first order by AMOC changes. However, the AMOC does decrease in these simulations (by $\sim 40\%$ in RCP4.5 and by $\sim 90\%$ in RCP8.5) due to other climatic changes.

Figure 2 illustrates the combined effects of warming and GIS melting on surface salinities. Subpolar surface waters

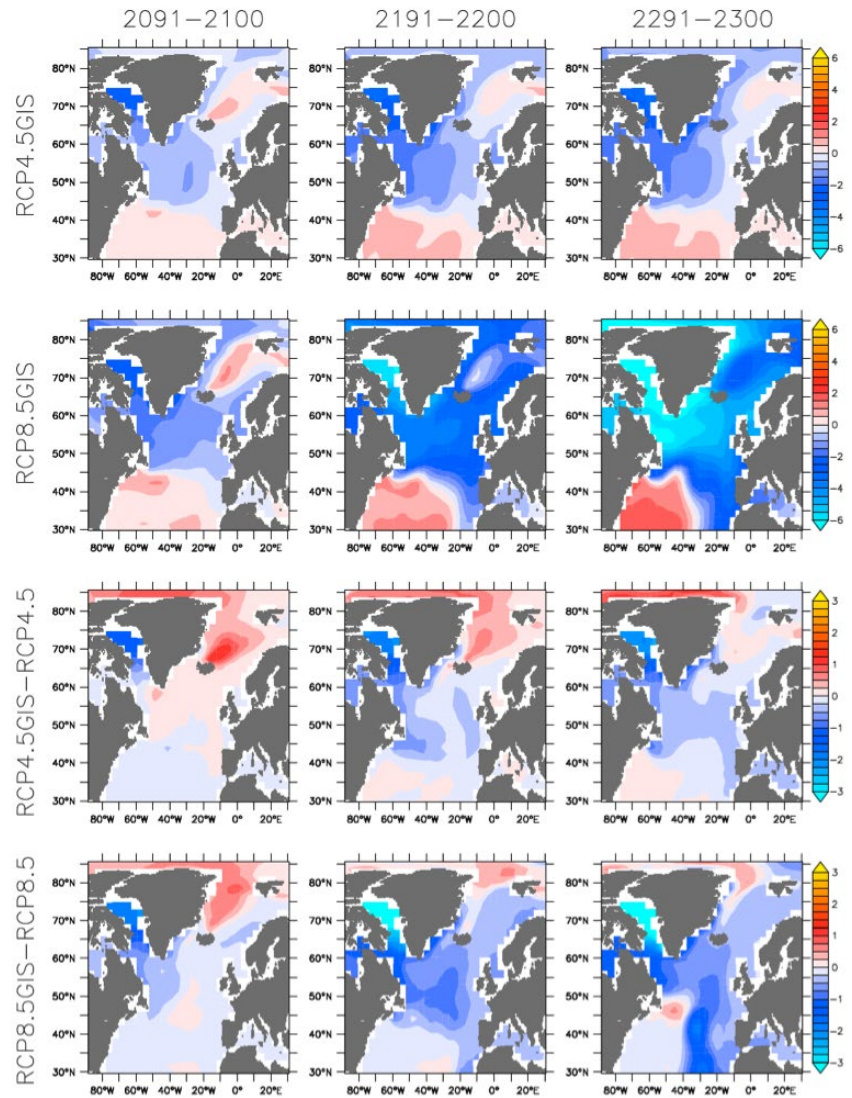


Figure 2: Surface salinity changes relative to the end of the 20th century (1991-2000) simulated by the OSU Vic model for the end of the 21st (left), 22nd (center) and 23rd (right) centuries for the RCP4.5GIS (top) and RCP8.4GIS (second from top) scenarios. The third and fourth rows show the effect of GIS melt alone by subtracting the results from the corresponding simulations without ice melt.

freshen by 0.1-0.2 (salinity is unitless but the numbers are comparable to earlier units such as g/kg or practical salinity units) for RCP4.5GIS with largest amplitudes in the western parts of the basin such as the Labrador Sea. Freshening intensifies until about year 2200 after which it stays approximately constant. The subtropical gyre salinifies by ~0.05 mostly during the 22nd century due to the intensified atmospheric hydrological cycle. Manabe and Stouffer observed this same pattern in their work.

In RCP8.5GIS the same pattern is found albeit with intensified amplitudes. The subpolar gyre continues to freshen during the 23rd century reaching values of more than 5 units lower, whereas the subtropical gyre salinifies by 0.1-0.15 units. GIS melting contributes to the freshening particularly around Greenland but it is less important than the intensification of the atmospheric hydrological cycle, consistent with Manabe and Stouffer's findings.

Also in line with their analysis, the subpolar gyre is consistently the region of minimum warming (Figure 3). This is true for both emission scenarios and all time periods considered and does not appear to be strongly affected by GIS melt. GIS melt seems to have mostly a cooling effect on surface temperatures in RCP4.5 for all considered time periods and for RCP8.5 at the end of the 21st century particularly along the southeast coast of Greenland, consistent with earlier results (Lenaerts et al. 2015). Cooling would be consistent with the effects of increased stratification and reduced convection, which leads to interior warming and cooling at the

surface. However, in the Nordic Seas, GIS melt results in warming in this model, in line with others (Swingedouw et al. 2013), who attributed it to advection of subsurface heat anomalies from the subpolar gyre. During the 22nd and 23rd centuries in the RCP8.5 scenario GIS melt in the OSU Vic model leads to warming throughout the North Atlantic with a minimum in the subpolar gyre, hence amplifying the pattern from warming alone. This warming response to GIS melt is model dependent. The only other

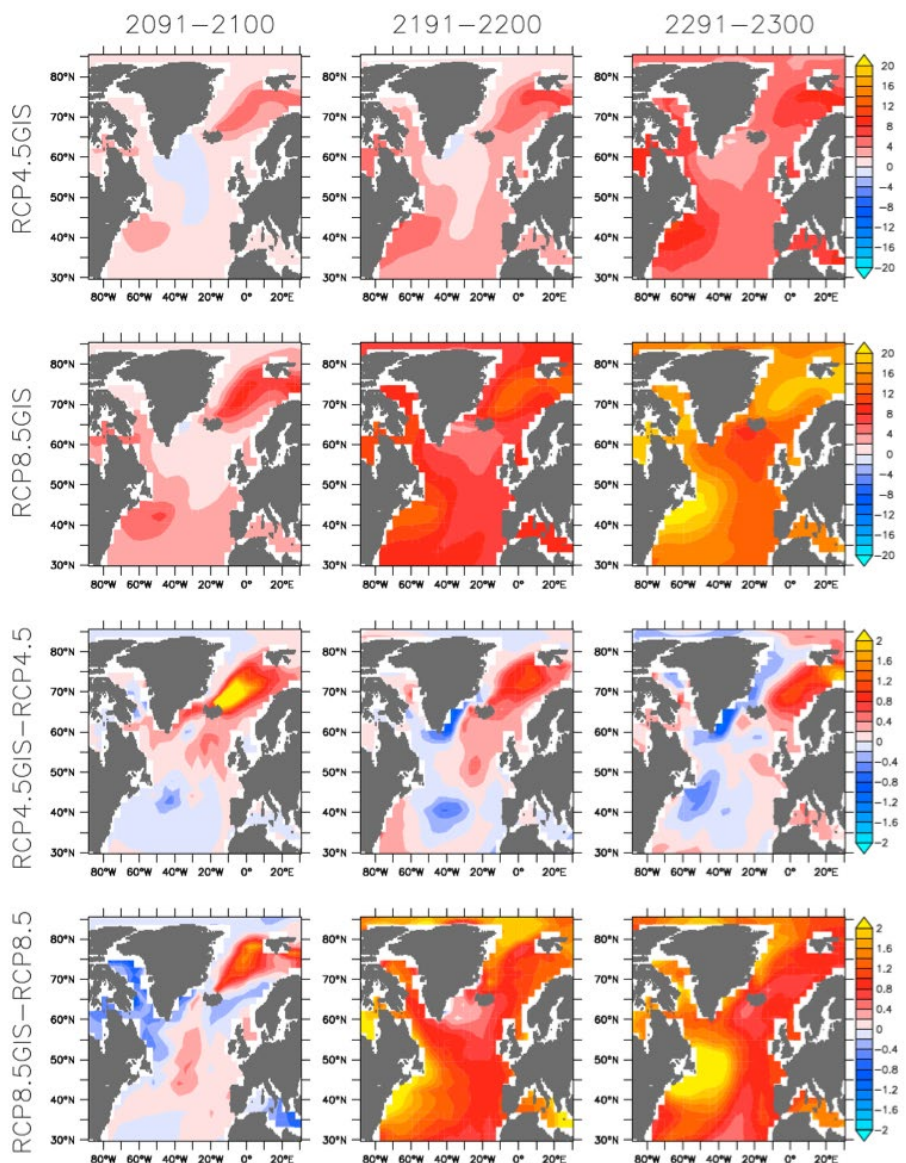


Figure 3: As Figure 2, but for sea surface temperature (°C).

model for which data for this scenario and time were readily available (CCSM3) does not show a comparable warming. The reasons for the warming and for the model dependency are currently not understood. They may be related to reduced uptake of anthropogenic heat due to enhanced stratification, but this remains speculative at this point. It would be useful to examine other models to evaluate robustness across models. More analysis will be required to better understand the surface temperature response to GIS melt.

Discussion

Our results suggest that surface meltwater fluxes from Greenland projected for the end of this century (~ 0.01 Sv) for an intermediate emission scenario (RCP4.5) will have only a relatively small impact on sea surface temperatures. This is in contrast with recent speculations that melting of the GIS during the 20th century (~ 0.003 Sv) has already affected sea surface temperatures in the North Atlantic and the AMOC (Rahmstorf et al. 2015). Therefore we think that GIS meltwater fluxes are unlikely to have influenced either the warming hole or the cold blob. However, we have neglected changes in marine ice loss due to calving icebergs or subsurface melting of marine terminating glaciers, which are difficult to project. Based on observational estimates from the last two decades of the 20th century a relation has been suggested between surface melting and marine ice loss due to processes such as ice warming and softening, basal lubrication, and increased circulation below and heat flux to ice shelves (Box and Colgan 2013). If this correlation would hold over multiple decades to centuries it could approximately double the freshwater fluxes estimated here, which would imply also larger impacts on AMOC and climate. However, even though solid ice discharge has been observed to have increased during recent decades, its increase from 2000 to 2012 was less than the increase in surface runoff, supporting the idea that surface melt will dominate future mass loss on decadal and longer timescales (Enderlin et al. 2014).

Outlook

Future efforts to improve model-based estimates of ice sheet mass loss on climate require better understanding of these processes and how they would change with a changing climate, with the ultimate goal to include quantitative parameterizations in global climate models. Here we have only considered the Greenland ice sheet but similar considerations apply to the Antarctic ice sheet. Large meltwater fluxes from the ice sheets have the potential to trigger large climate impacts as illustrated recently by Hansen et al. (2016). Physics based constraints on these fluxes are needed for more realistic assessments of their impacts. Continued monitoring of both ice sheets as well as the surrounding oceans and atmosphere is essential to improve and better evaluate existing models. New climate models that include interactive ice sheets and ice shelves will be required for a more comprehensive understanding of feedbacks between the ocean-atmosphere system and the cryosphere. Ongoing efforts such as the [Marine Ice Sheet-Ocean Model Intercomparison Project](#) may foster this goal.

Even though it is known that meltwater input to the surface ocean will lead to increased stratification and reduced mixing with deeper, nutrient rich waters, very few studies have investigated the impacts on phytoplankton productivity and the marine ecosystem or on biogeochemical cycles such as those of carbon and oxygen. Such studies will be needed if we want to get a more complete assessment of the possible future consequences of anthropogenic carbon emissions.

References

- Box, J. E., and W. Colgan, 2013: Greenland ice sheet mass balance reconstruction. Part III: Marine ice loss and total mass balance (1840–2010). *J. Climate*, **26**, 6990–7002, doi: [10.1175/JCLI-D-12-00546.1](https://doi.org/10.1175/JCLI-D-12-00546.1).
- Cheng, W., J. C. H. Chiang, and D. X. Zhang, 2013: Atlantic Meridional Overturning Circulation (AMOC) in CMIP5 models: RCP and historical simulations. *J. Climate*, **26**, 7187–7197, doi: [10.1175/JCLI-D-12-00496.1](https://doi.org/10.1175/JCLI-D-12-00496.1).
- Enderlin, E. M., I. M. Howat, S. Jeong, M. J. Noh, J. H. Angelen, and M. R. Broeke, 2014: An improved mass budget for the Greenland ice sheet. *Geophys. Res. Lett.*, **41**, 866–872, doi: [10.1002/2013GL059010](https://doi.org/10.1002/2013GL059010).
- Gregory, J. M., 2005: A model intercomparison of changes in the Atlantic thermohaline circulation in response to increasing atmospheric CO₂ concentration. *Geophys. Res. Lett.*, **32**, doi: [10.1029/2005GL023209](https://doi.org/10.1029/2005GL023209).
- Hansen, J., and Coauthors, 2016: Ice melt, sea level rise and superstorms: evidence from paleoclimate data, climate modeling, and modern observations that 2 °C global warming could be dangerous. *Atmos. Chem. Phys.*, **16**, 3761–3812, doi: [10.5194/acp-16-3761-2016](https://doi.org/10.5194/acp-16-3761-2016).
- Hu, A., G. A. Meehl, W. Han, and J. Yin, 2009: Transient response of the MOC and climate to potential melting of the Greenland Ice Sheet in the 21st century. *Geophys. Res. Lett.*, **36**, doi: [10.1029/2009GL037998](https://doi.org/10.1029/2009GL037998).
- Hu, A. X., G. A. Meehl, W. Q. Han, and J. J. Yin, 2011: Effect of the potential melting of the Greenland Ice Sheet on the Meridional Overturning Circulation and global climate in the future. *Deep-Sea Res Pt II*, **58**, 1914–1926, doi: [10.1016/j.dsret.2010.10.069](https://doi.org/10.1016/j.dsret.2010.10.069).
- Lenaerts, J. T. M., D. Le Bars, L. van Kampenhout, M. Vizcaino, E. M. Enderlin, and M. R. van den Broeke, 2015: Representing Greenland ice sheet freshwater fluxes in climate models. *Geophys. Res. Lett.*, **42**, 6373–6381, doi: [10.1002/2015GL064738](https://doi.org/10.1002/2015GL064738).
- Manabe, S., and R. J. Stouffer, 1993: Century-Scale Effects of Increased Atmospheric CO₂ on the Ocean-Atmosphere System. *Nature*, **364**, 215–218, doi: [10.1038/364215a0](https://doi.org/10.1038/364215a0).
- Manabe, S., and R. J. Stouffer, 1994: Multiple-century response of a coupled ocean-atmosphere model to an increase of atmospheric carbon dioxide. *J. Climate*, **7**, 5–23, doi: [10.1175/1520-0442\(1994\)007<0005:MCROAC>2.0.CO;2](https://doi.org/10.1175/1520-0442(1994)007<0005:MCROAC>2.0.CO;2).
- Mikolajewicz, U., M. Vizcaino, J. Jungclaus, and G. Schurgers, 2007: Effect of ice sheet interactions in anthropogenic climate change simulations. *Geophys. Res. Lett.*, **34**, doi: [10.1029/2007GL031173](https://doi.org/10.1029/2007GL031173).
- Rahmstorf, S., J. E. Box, G. Feulner, M. E. Mann, A. Robinson, S. Rutherford, and E. J. Schaffernicht, 2015: Exceptional twentieth-century slowdown in Atlantic Ocean overturning circulation. *Nat. Climate Change*, **5**, 475–480, doi: [10.1038/nclimate2554](https://doi.org/10.1038/nclimate2554).
- Rahmstorf, S., and Coauthors, 2005: Thermohaline circulation hysteresis: A model intercomparison. *Geophys. Res. Lett.*, **32**, doi: [10.1029/2005GL023655](https://doi.org/10.1029/2005GL023655).
- Rignot, E., I. Velicogna, M. R. van den Broeke, A. Monaghan, and J. T. M. Lenaerts, 2011: Acceleration of the contribution of the Greenland and Antarctic ice sheets to sea level rise. *Geophys. Res. Lett.*, **38**, doi: [10.1029/2011GL046583](https://doi.org/10.1029/2011GL046583).
- Schmittner, A., M. Latif, and B. Schneider, 2005: Model projections of the North Atlantic thermohaline circulation for the 21st century assessed by observations. *Geophys. Res. Lett.*, **32**, doi: [10.1029/2005GL024368](https://doi.org/10.1029/2005GL024368).
- Schmittner, A., T. A. Silva, K. Fraedrich, E. Kirk, and F. Lunkeit, 2011: Effects of mountains and ice sheets on global ocean circulation. *J. Climate*, **24**, 2814–2829, doi: [10.1175/2010JCLI3982.1](https://doi.org/10.1175/2010JCLI3982.1).
- Swingedouw, D., and P. Braconnot, 2007: Effect of the Greenland Ice-Sheet melting on the response and stability of the AMOC in the next centuries. *Ocean circulation: mechanisms and impacts*, A. Schmittner, J. C. H. Chiang, and S. R. Hemming, Eds., American Geophysical Union, doi: [10.1029/173GM24](https://doi.org/10.1029/173GM24).
- Swingedouw, D., P. Braconnot, and O. Marti, 2006: Sensitivity of the Atlantic Meridional Overturning Circulation to the melting from northern glaciers in climate change experiments. *Geophys. Res. Lett.*, **33**, doi: [10.1029/2006GL025765](https://doi.org/10.1029/2006GL025765).
- Swingedouw, D., C. B. Rodehacke, S. M. Olsen, M. Menary, Y. Q. Gao, U. Mikolajewicz, and J. Mignot, 2015: On the reduced sensitivity of the Atlantic overturning to Greenland ice sheet melting in projections: a multi-model assessment. *Climate Dyn.*, **44**, 3261–3279, doi: [10.1007/s00382-014-2270-x](https://doi.org/10.1007/s00382-014-2270-x).
- Swingedouw, D., and Coauthors, 2013: Decadal fingerprints of freshwater discharge around Greenland in a multi-model ensemble. *Climate Dyn.*, **41**, 695–720, doi: [10.1007/s00382-012-1479-9](https://doi.org/10.1007/s00382-012-1479-9).
- Weaver, A. J., and Coauthors, 2012: Stability of the Atlantic meridional overturning circulation: A model intercomparison. *Geophys. Res. Lett.*, **39**, doi: [10.1029/2012GL053763](https://doi.org/10.1029/2012GL053763).

ANNOUNCEMENTS

Webinar Series: A Tale of Two Blobs

**Tuesday, June 7
1:00 PM EDT / 10:00 AM PDT**

A Tale of Two Blobs, Part I: The warm blob of the North Pacific

Dillon Amaya, Scripps Institution of Oceanography
Samantha Siedlecki, U. Washington
Emanuele Di Lorenzo, Georgia Institute of Technology

**Friday, June 10
12:00 PM EDT / 9:00 AM PDT**

A Tale of Two Blobs, Part II: The cold blob of the North Atlantic

Steve Yeager, National Center for Atmospheric Research
Simon Josey, National Oceanography Centre, UK
Andreas Schmittner, Oregon State U.

Click to learn more



www.usclivar.org
uscpo@usclivar.org
twitter.com/usclivar

US Climate Variability and Predictability (CLIVAR) Program

1201 New York Ave. NW, Suite 400
Washington, DC 20005
(202) 787-1682

US CLIVAR Announces a New Working Group:

Changing Width of the Tropical Belt

US CLIVAR welcomes the following new members, who will help science planning and implementation of program goals. These new members bring a broad range of expertise across disciplines and research methods that complement and balance the current Panel membership.

Working Group Members

Kevin Grise, University of Virginia, co-chair
Paul Staten, Indiana University, co-chair

Ori Adam, ETH Zurich

Robert Allen, U. California-Riverside

Thomas Birner, Colorado State U.

Gang Chen, U. California-Los Angeles

Kerry Cook, U. Texas-Austin

Sean Davis, NOAA ESRL/U. Colorado

Qiang Fu, U. Washington

Kristopher Karnauskas, U. Colorado

James Kossin, NOAA NCEI

Chris Lucas, Bureau of Meteorology, Australia

Amanda Maycock, U. Leeds

Timothy Merlis, McGill U.

Xiao-Wei Quan, NOAA ESRL/U. Colorado

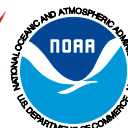
Karen Rosenlof, NOAA ESRL

Isla Simpson, National Center for Atmospheric Research

Caroline Ummenhofer, Woods Hole Oceanographic Institution

Darryn Waugh, Johns Hopkins U.

US CLIVAR acknowledges support from these US agencies:



This material was developed with federal support of NASA, NSF, and DOE (AGS-1502208), and NOAA (NA11OAR4310213). Any opinions, findings, conclusions, or recommendations expressed in this material are those of the authors and do not necessarily reflect the views of the sponsoring agencies.